UNIVERSITÀ DEGLI STUDI DI BRESCIA

DOTTORATO DI RICERCA IN BIOMEDICAL AND TRANSLATIONAL MEDICINE

MED/07

CICLO
XXXIII

ARV p17 SUPPRESSES ANGIOGENESIS BY PROMOTING DPP4 SECRETION

EKTA MANOCHA

Firma.

Prof. ARNALDO CARUSO

Firma.

Avian reovirus p17 suppresses angiogenesis by promoting DPP4 secretion

Contents

Abstract

Avian reovirus p17 (ARV p17) is a non-structural protein displaying no sequence similarity with other known proteins. It was shown to activate autophagy, interfere with gene transcription and induce a significant tumor cell growth inhibition *in vitro* and *in vivo*. In this study, we show the potent anti-angiogenic properties of ARV p17. The viral protein was found to significantly inhibit human umbilical vein endothelial cell (HUVEC) migration, capillary-like structure and new vessel formation. ARV p17 was not only able to suppress the EC physiological angiogenesis but also rendered ECs insensitive to two different potent pro-angiogenic inducers, such as VEGF-A and FGF-2. The anti-angiogenic activity of ARV p17 was also confirmed on primary human microvascular ECs. ARV p17 was found to exert its anti-angiogenic activity by upregulating transcription and release of the well-known tumor suppressor molecule DPP4. The ability of ARV p17 to impact on angiogenesis is completely new and highlights the "two compartments" activity of the viral protein that is expected to hamper the tumor parenchymal/stromal cross-talk. The complex antitumor activity of ARV p17 may open the way to a new promising field of research aimed to develop new therapeutic approaches for treating tumor and cancer metastasis.

Il reovirus aviario p17 (ARV p17) è una proteina non strutturale che non mostra alcuna somiglianza di sequenza con altre proteine note. È stato dimostrato che attiva l'autofagia, interferisce con la trascrizione genica e induce una significativa inibizione della crescita delle cellule tumorali in vitro e in vivo. In questo sudio, mostriamo le potenti proprietà anti-angiogeniche di ARV p17. È stato scoperto che la proteina virale inibisce in modo significaivo la migrazione delle cellule endoteliali dela vena ombelicale umana (HUVEC), la struttura capillare e la formazione di nuovi vasi. L,ARV p17 non solo è stato in grado di sopprimere l'angiogenesi fisiologica dell'EC, ma ha anche reso gli EC insensibili a due diversi potenti induttori pro-angiogenici, come VEGF-A e FGF-2. L'attività anti-angiogenica di ARV p17 è stata confermata anche su EC microvascolari umane primarie. È stato riscontrato che l'ARV p17 esercita la sua attività anti-angiogenica sovraregolando la trascrizione e il impatto sull'angiogenesi è completamente nuova ed evidenzia l'attività dei "due compartimenti" della proteina virale che dovrebbe ostacolare il cross-talk parenchimale/stromale del tumore, La complessa attività antitumorale di ARV p17 può aprire la strada a un nuovo promettente campo di ricerca volto a svillupare nuovi approcci terapeutici per il trattamento di tumori e metastasi tumorali.

1. INTRODUCTION

Tumor angiogenesis is regulated by a complex network of morphogenetic and molecular pathways controlled by membrane-bound proteins, as well as soluble factors, including VEGF, TGF-β, bFGF, MMP-2, and MMP-9. Restoring perfusion to ischemic organs or limbs is a goal of therapeutic angiogenesis, while positive outcome with anti-angiogenic therapy has been a target for the treatment of tumors. Cell-cell adhesion in endothelial cells is largely mediated by VE-cadherin, a transmembrane protein that allows endothelial cells to regulate barrier function essential for angiogenesis. Deletion of VE-cadherin can abolish transmission of key remodeling and maturation signals via VEGFR-2 as their association has been suggested as an essential mechanosensor in response to shear flow. Endothelial cell sprouting and tubule formation is another way for the cells to remodel their environment, often by secretion of endogenous enzymes. The interplay between VE-cadherin and VEGFR-2 expression during spheroid formation indicates that increasing initial cell-cell contacts may enhance the responsiveness of microvascular endothelial cell spheroids to proangiogenic cues, which are delivered as recombinant growth factors or in conjunction with other cells secreting paracrine factors [1]. VE-cadherin expression disappears during the angiogenic process to increase the motility capacity of the activated endothelial cells whereas N-cadherin expression, essential for interactions between endothelial and mural cells for stabilization of nascent blood vessels by mural cells, is upregulated. During sprouting angiogenesis, Notch signaling plays a central role in the coordination of cellular behaviors on "stalk" growing cells and on "tip" leading endothelial cells through the modulation of VEGF-mediated angiogenesis. The critical existence of a balance between Delta and Jagged-mediated Notch signaling has been proposed to control the endothelial cell fate such as cell proliferation, survival/apoptosis, migration, and cell differentiation as Jagged 1 competition with Dll-4 would result in partial inhibition of Dll4-mediated signaling and promotion of angiogenesis through enhanced sprouting of endothelial cells, possibly via mechanisms mediating cell migration and cell proliferation involving ERK1/2 MAPK pathway, lipid raft-associated γ-secretase activity and MAPK p38 or JNK pathway [2].

Recently, tumor-derived exosomes (TEX), virus-size vesicles, which circulate freely throughout body fluids and accumulate in the tumor microenvironment, have been recognized as a new contributor to angiogenesis. TEXs have been reported to induce phenotypic and functional changes in endothelial cells, including pericytes. Pericytes have diverse functions including the

guidance of sprouting tubes, the sense of angiogenic stimuli, and mainly the stabilization of vessels. They reflect the status of a mature vessel and are therefore heavily involved in the angiogenic process. For solid tumors, an adequate blood supply is of critical importance for the development, growth, and metastasis. The preparation of the tumor microenvironment by TEX could pave the way for the initial tumorigenesis and the subsequent tumor progression, including accelerated angiogenesis [3]. Cell aggregates, known as spheroids, provide a promising alternative to individual cells, as they mimic the cell-cell contacts necessary for angiogenesis. Unlike individual cells that are separated from their endogenous extracellular matrix (ECM) following trypsinization, spheroids retain this instructive ECM during culture and transplantation. Spheroids formed of human mesenchymal stem cells (MSC) exhibit enhanced therapeutic potential with greater resistance to apoptosis compared to individual cells. Spheroid formation with endothelial cell populations to promote microvessel formation has been established in both *in vitro* and *in vivo* models.

Perturbations in cell growth are one of the characteristics of animal virus infections that contribute to the pathogenesis process. There is compelling evidence from *in vivo* and *in vitro* studies that collagen promotes capillary morphogenesis through integrin signaling. It has been shown that collagen type I can initiate the early stages of angiogenesis, including initial EC retraction followed by shape change to a spindle-like morphology, alignment, and connection into precapillary cross-like structures; tubes then form by a process of vacuolation leading to alterations in cell shape, contractility, and polymerization and arrangement of cytoskeletal actin into stress fibres. Many of the known ECM inhibitors of angiogenesis exert their effects by perturbing integrin binding and signaling pathways, including endorepellin, arresten, tumstatin, endostatin, and canstatin [4]. Such ECM inhibitors in the form of viral proteins could prove to provide a safe and efficient oncotherapy.

Studies conducted on oncolytic reovirus delivery to cancer patients revealed that the virus is largely found in hematopoietic cells, specifically mononuclear cells, granulocytes, and platelets. Endothelial cells also function as sites of amplification for many viruses that spread via the bloodstream. e.g. BTV (Bluetongue virus), a member of the Reoviridae family, which infects and replicates in mononuclear cells, lymphocytes, and endothelial cells, acquires endothelial JAM-A

expression for the entry into and exit from the blood stream [5]. This property of reoviruses could be exploited for their use in effective virotherapy. Cancer cells release many growth factors, and physical interactions between the tumor and the endothelium that stimulates endothelial cells to differentiate and remodel, as shown by Chiew et al, in a hepatocellular carcinoma model [6]. In light of these observations, previously, we reported that expression of U94, an HHV-6 protein, strongly inhibited angiogenesis in both lymphatic endothelial and vascular endothelial cells [7]. With the growing revelation of new oncolytic viruses, there is also an emergence to explore the viral proteins which could suppress the angiogenic and metastatic activities of the cancer cells.

Several non-structural Rep proteins, known for their involvement in virus replication cycle and latency, have been characterized from different parvoviruses for their human-amicable roles like AAV Rep-68/78, which has been shown to possess anticancer properties via cell cycle regulation [8] and has homologous counterparts in other viruses like human herpes virus HHV-6A Rep 6 (U94) that also shares the functional activity with Rep-68/78 [9], possibly due to the integration of an ancestral parvovirus into the genome of an ancestral betaherpesvirus during coinfection [10]. Avian parvoviruses like BDPV (Barbarie Duck parvovirus), MDPV (Muscovy Duck parvovirus), and GPV (Goose Parvovirus) are the closest relatives of AAV-Rep 68 [10] and encodes another NS protein, namely Rep 1/2 which exerts NTP-dependent helicase activity [11]. In light of these pieces of evidence, we investigated one of the avian viral non-structural protein p17 from avian reovirus, widely known for its role in cancer suppression and cell growth retardation, to explore its property of regulating angiogenesis in human macrovascular and microvascular endothelial cells.

Avian Reoviruses (ARVs) are important pathogens, belonging to the Orthoreovirus genus in the Reoviridae family, associated with different diseases, like viral arthritis, enteric disease problems, immunosuppression, and chronic respiratory disorders in many avian species [12]. The ARV genome consists of 10 double-stranded RNA-genome segments, which encode at least 10 structural proteins and four nonstructural proteins, but very little is known about the functions of most proteins. The non-structural p17 protein of ARVs (ARV p17) is a 146 aa protein encoded by the S1 gene segment, whose ORF is highly conserved in all avian Reovirus S1 segments and has been suggested to play an important role in virus-host interactions [13]. The ARV p17 doesn't

show sequence similarity with any other known protein, so its sequence offers no clues about its function [14]. It is known to be a nucleocytoplasmic shuttling protein, which has been suggested to participate in cell nuclear processes, such as gene transcription, DNA binding, and cell growth regulation [15,16]. The viral protein possesses the capability to translocate into the nucleus by the presence of a nuclear localization signal (NLS) and its nuclear localization is correlated with autophagy induction and an increase of viral replication [17] by regulating p53/PTEN/mTORC1, AMPK, and PKR/eIF2α signaling pathways[18]. Recently, Huang et al. showed that ARV p17 suppresses the Tpr nucleoprotein leading to the nuclear accumulation of p53 and p21 and, consequently, to PTEN activation. This allows ARV p17 to impair the cell cycle progression through Tpr/p53/PTEN/Akt and Tpr/p53/p21 signaling pathways [19]. Indeed, different studies have reported the capability of ARV p17 to promote significant cell growth inhibition and cell cycle retardation in several cancer cell lines through activation of the p53 pathway and interaction with CDKs and cyclins [20]. In particular, the direct interaction of ARV p17 with CDK1 leads to its inactivation, but also to the suppression of Plk1 by activating the Tpr/p53 and ATM/Chk1/PP2A pathways and participating in cdc25C degradation via a ubiquitin-proteasome pathway [21].

To summarize, modulation of cell growth is a common feature of different animal viruses, which alters the physiology of the host to enhance its own replication. Several viral proteins from human and mammalian viruses, such as HSV ICP0 [22,23], EBV Zta transcription factor [24], M-CoV non-structural protein p28 [25]and HTLV-1 Tax protein [26], are able to induce cell cycle arrest. Moreover, non-structural proteins involved in regulating virus replication cycle and latency, such as AAV Rep-68/78 and HHV-6A Rep 6 (U94), have been characterized for their anticancer properties. These findings have paved the way to study viruses that normally live in and among us for genetic blueprints that enables them to make molecules that act like drugs and might serve as the basis for new human anticancer therapeutics [27]. Tumor growth, progression, and metastasis are driven by angiogenesis [28,] and inhibition of angiogenesis has become one of the most exciting approaches in the development of anticancer therapy. At present, despite the involvement of ARV p17 in arresting cell growth and tumorigenesis, a possible role of the viral protein in modulating EC (endothelial cell) proliferation and angiogenic activity has not yet been explored. In this study, we investigated the properties of ARV p17 in regulating angiogenesis and

vasculogenesis, and demonstrate that the viral protein is able to significantly inhibit macrovascular and microvascular EC migration, capillary-like structure, and new vessel formation. ARV p17 activity occurred in the absence of EC toxicity. Moreover, we show the capability of ARV p17 to suppress either the physiological or VEGF- and FGF-induced angiogenesis. Finally, we highlight that the viral protein exerts its anti-angiogenic activity on both macrovascular and microvascular ECs and that occurs through an increase in DPP4 secretion.
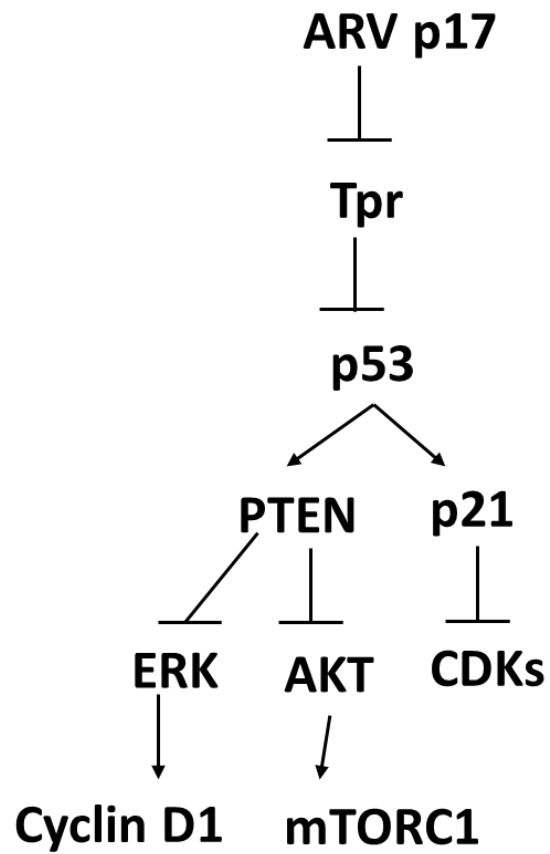
Huang et al., 2015 Schematic representation displaying major signaling pathways regulated by p17 protein from avian reovirus in various cell lines like Vero, DF-1 and HeLa.

2. STATE OF THE ART

Background

Avian Reovirus belongs to the genus Orthoreovirus in the family Reoviridae has a double-stranded 10-segmented RNA genome. The genome segments encode at least eight structural and four non-structural proteins. p17 is a 17-kDa non-structural protein encoded by the S1 gene and contains 146 amino acids [13]. The S1 genome segment of ARV contains three open reading frames that translate into p10, p17, and σC proteins, respectively. p10 displays membrane destabilization activity [29-31], σC is known to be a cell attachment protein [32] capable of inducing apoptosis [33-35] and p17 is a nucleocytoplasmic shuttling protein. Previous studies have shown that p17 has a basic region, [119]IAAKRGRQLD[128], which is similar to the functional monopartite NLS of the c-Myc protein and is highly conserved in the different ARV isolates [16]. A monopartite-type functional NLS near the C terminus of p17 is necessary for nuclear import and interacts with nucleoporin Tpr localized within the nuclear basket of the nuclear pore complex (NPC), which suppresses Tpr, thereby activating cell cycle regulators like p53, PTEN, and p21 followed by downregulation of PI3K/AKT/mtor and ERK signaling pathways [19,36]. Previous studies showed that p17 causes deactivation of eIF4E, eIF4G, and eIF4B, leading to mTORC1 and downstream protein synthesis [37]. Besides, it has been shown that ectopic expression of p17 results in the retardation of cell growth by activating the p53 pathway [17]. Chi *et al.* showed that ARV p17 induces autophagy and regulates this process through the p53/PTEN/mTORC1, AMPK, and PKR/eIF2α signaling pathways. They also demonstrated that p17 nuclear localization is responsible for inducing autophagy; since the latter is delayed and viral replication is affected when the protein could not enter the nucleus [38]. In a recent report, Chiu *et al.* identified that N-terminal 21 amino acids (aa 19 to 40) of p17, containing a nuclear export signal, [19]LSLRELAI[26], is required for interaction with hnRNP A1 which serves as a carrier protein in mediating nucleocytoplasmic shuttling. While lamin A/C mediates p17 nuclear import, p17-hnRNP A1 carrier-cargo complex interacts with lamin A/C and nucleoporin Tpr via its NLS thereby transcriptionally downregulating Tpr and activating p53, PTEN, and p21, enhancing virus replication [19].

ARV p17 has been observed to induce cell growth retardation, cell cycle arrest, and host cellular translation shutoff by suppression of CDK1 and PLK1 like signaling pathways and regulation of p53/PTEN/mTORC1 like pathways [20]. Since, ARV p17 is known to induce autophagy and

activate protein kinase RNA-activated signaling, therefore, leading towards the activation of the innate immune system, and mount the immune response against tumors. In summary, p17 happens to facilitate virus replication via induction of cell cycle arrest and cellular translation shutoff [17,19,38] and thus diverting the cellular machinery required for normal cell-cycling processes for virus replication [21] and mediating immune responses. Secondly, ARV p17 positively regulates phosphatase and tensin deleted on chromosome 10 (PTEN), AMP-activated protein kinase (AMPK), and dsRNA-dependent protein kinase RNA (PKR)/eIF2 signaling pathways, accompanied by downregulation of Akt and mammalian target of rapamycin complex 1 (mtor1), thereby triggering autophagy [39].

Role in cell cycle

P17 exhibited cell growth inhibition and cell cycle retardation in multiple avian, mammalian, and cancer cell lines like Vero, DF-1, human adenocarcinoma (SW620), human cervical cancer (HeLa), lung cancer (A549), and reduced tumor size *in vivo* [20]. Mainly, p17 suppressed CDK1 function by suppressing both PLK1 and CDC25C to cause phosphorylation of CDK1. The viral protein was shown to compete with cyclin B1 to bind CDK1, leading to CDK1 retention and prevention of the cyclin B1/CDK1 complex in the nucleus leading towards G2/M cell cycle retardation. Moreover, ARV infection or p17 transfection is found to be responsible for p53 and PTEN phosphorylation hence impairing the targeting ability of E3 and MDM2 ubiquitin ligases respectively. This causes enhancement of p53/cyclin H interaction which, in turn, mediates suppression of CAK activity by p17, dissociating CDK7/Cyclin H complex. In the same study, Chiu *et al*. reported that a particular motif in p17 protein [140]WXFD[143] and residues D113 and K122 are conserved across different strains and are critical for CDK2 and CDK6 binding. To conclude, p17 suppressed the formation of CDK1/cyclin A2, CDK2/cyclin E1 and CDK6/cyclin D1 complexes by directly binding to CDK, cyclin, or CDK/cyclin complexes, benefitting virus replication. P17 was shown to downregulate CDK1 through two independent pathways: PI3K/AKT and Tpr/p53/PTEN/ERK or Tpr/p53/PTEN-dependent inhibition of mtorc1 pathway.

Avian reovirus ORF and protein purification

The S1 gene of avian reovirus is reported to encode three partially overlapping ORF's as per the data extracted from the strain S1133 [32]. The larger portions of ORF1 encoding p10 are present in the supernatant fraction and have been purified from the supernatant by an MBP gene fusion vector on an amylose-agarose column. Sigma C, on the other hand, is a structural protein and is found to be localized in the plasma membrane of transfected cells [40]. Both p10 and p17 are membrane-associated proteins whereas sigma C is present in the soluble fraction and intracellular expression of p10 induces syncytium formation in BSC-40 monkey cells [13] and induces cell-cell fusion. There is no significant homology been revealed between p17 and any other known protein, except its homologs from other avian reovirus strains and Nelson Bay virus. At the same time, the fact that these proteins are specified by out of phase reading frames suggests that p10, p17, and sigma-C are structurally and functionally unrelated to one another.

The recombinant protein ARV p17 is found to be present in inclusion bodies and not in the soluble form in the prokaryotic expression vector system. It has been attempted to be purified previously by several means, as reported, with the help of guanidine hydrochloride (6 M) followed by dialysis or in the presence of a His-tag by affinity chromatography using a Ni-NTA resin [30]. Here, we have purified the GST-tagged ARV p17 recombinant protein in the presence of urea (6 M) by affinity chromatography using a gluthatione-sepharose resin. Since it has been difficult to purify recombinant proteins from inclusion bodies in their native form; we have purified p17 with a GST tag present at the N-terminus to increase the stability of the molecule. Previously, U94/Rep 6, another viral protein from HHV-6A has been purified from the insoluble fraction under denaturing conditions on a hydroxyapatite column with 95% purity and utilized for the characterization and studying the role of the protein in suppressing carcinogenic activities [20].

Other non-structural Rep proteins from mammalian viruses

- Parvovirus NS1

Several candidate oncolytic viruses are under investigation including herpes simplex virus, adenovirus, and autonomous parvoviruses [42]. Parvovirus H-1 is an autonomous parvovirus,

single-stranded non-enveloped DNA virus, of rat origin and is shown to be capable of selectively inhibiting malignant transformation and neoplastic growth of cells from cells of both animal and human origin [43,44]. Furthermore, infection of humans by parvovirus appeared to be harmless. The viral non- structural protein NS1 is a key regulator of the parvoviral life-cycle through its multiple activities, including adenosine triphosphate binding and hydrolysis, oligomerization, site-specific DNA binding, site-specific and strand-specific DNA nicking, helicase function, and capacity for promoter trans-regulation. The intracellular accumulation of NS1 protein, owing to its bipartite NLS sequence, is a major effector of virus-induced cytotoxicity of the neoplastic cells [45]. Moreover, modification of specific residues is important for the toxicity of the protein (Thr-435 and Ser-473) even though it is not responsible for the subcellular localization of the protein [46]. These properties enable NS1 to control a variety of processes that are necessary for progeny particle production including viral DNA amplification and gene expression. Thus, NS1 cytotoxicity may result, at least in part, from the dysregulation of intracellular signaling pathways [47]. Cell death caused by NS1 was shown to be induced by apoptosis and dependent on caspase-3. The cytostatic potential of NS-1 was mediated by an accumulation of cells in the G2 phase and a block in cellular DNA replication was suggested to be an end result of NS-1-induced damage [48]. Furthermore, H-1PV-induced cell death is mediated by NS1 through the accumulation of reactive oxygen species, which leads to oxidative stress, mitochondrial outer membrane permeabilization, DNA damage, cell cycle arrest, and finally, caspase activation [49].

- AAV Rep 68/78

AAVs, another member of the parvovirus family, a group of small single-stranded DNA, non-enveloped viruses belonging to the genus *Dependoparvovirus*, rely on helper viruses like adenoviruses or herpesviruses for their efficient replication [50]. The autonomous and helper-dependent parvoviruses have unique biological properties in common. Members of both groups efficiently suppress tumor growth in animals, irrespective of the mode of tumor induction [51]. The rep proteins, a family of multifunctional nonstructural AAV proteins, are required not just for AAV DNA replication but also for gene regulation. AAV Rep78 may inhibit the utilization of cAMP pathways by helper viruses and thereby inhibit productive replication of the helper virus [52]. In the early 1990s, AAVs were reported to inhibit not only carcinogen-induced SV40 DNA amplification [53] but also carcinogen-induced resistance against methotrexate, which has been

associated with the amplification of the DHFR (dihydrofolate reductase) gene. Rep78 is interfering with both SV40 DNA amplification and HSV ori_s replication possibly by directly interacting with HSV replication and amplification complex [51]. p53 levels were observed to be stabilized by AAV in adenovirus-infected cells. The interaction of AAV Rep78 with p53 was suggested to be responsible for the observed protection of p53 which is degraded by ubiquitination followed by interaction of adenoviral E1B, an early gene product, with p53. By protecting p53 from ubiquitin-mediated degradation by adenovirus, the function of p53 as a cell cycle blocking agent is restored in the presence of Rep78 [54].

Both AAV and HPV (human pappiloma virus) are cutaneous tissue-tropic viruses, productively replicating in differentiating keratinocytes. E7 of HPV interacts with c-Jun along with E7 interaction with pRb, to upregulate viral activity and deregulating cell-cycle control leading to malignant transformation. Elevated levels of c-Jun activity advance the G1 phase of the cell cycle by transactivating the promoter of cyclin D1. Rep78 has been shown to bind c-Jun both *in vitro* and *in vivo* in yeast and this association downregulates transcription from AP-1-dependent promoters. Furthermore, Rep78 alters c-Jun dependent transcription by inhibiting c-Jun binding to needed transcriptional partners/cofactors such as c-Fos, possibly through steric inhibition [55]. Rep78 interacts with PRKX (a homolog of cAMP-dependent PKA) and PKA and inhibits their kinase activities and block the induction of CREB-dependent transcription by reducing CREB phosphorylation in HeLa cells. A number of viruses have subsumed PKA/CREB pathways to regulate their gene expression; examples including HTLV 1, HIV 1, adenovirus, HSV, and EBV.

Rep78 has been observed to exert anti-proliferative effects on cells by blocking the cell cycle in all of the phases or by inducing apoptosis independently of p53 via the caspase-3 dependent pathway. It's binding to the cell cycle regulatory phosphatase cdc25A prevents the latter access to substrates Cdk1 and Cdk2 resulting in the inactivation of CDKs that are required for continued DNA replication along with the DNA damage induced by the nicking activity of Rep78 [56]. On the other hand, AAV2 anti-carcinogenic activities were further explored and AAV2 infection of MDA-MB-231 cells was found to induce increased S-phase entry, hypophosporylated pRb, and downregulation of p21 levels to facilitate the breast cancer cells for apoptosis by caspase-8 and -9 cleavage in the absence of PARP cleavage, thereby indicating a further switch to necrosis [57].

- Rep 6/U94

HHV-6 is a double-stranded DNA β-herpesvirus related to HCMV, exists as two closely related variants, HHV-6A and HHV-6B, known to be lymphotropic in nature. HHV-6/U94 gene is highly conserved in all HHV-6 strains has single-stranded DNA binding activity, might be involved in DNA replication, and is expressed at low levels during the early phases of viral replication [58]. U94 is known as a negative regulator of viral replication and T-cell lines stably expressing U94 do not support productive viral replication, owing to its high structural and functional similarity with AAV-2 Rep78/68 [9]. Since U94 mRNA is detected in the PBMCs from latently infected healthy individuals, our group proposed that U94 can be considered as a molecular marker of viral latency [59].

U94 is expressed at low levels during productive *in vitro* infection but is detected during viral latency. It was reported that high levels of U94 inhibit HHV-6 replication [7].U94 was able to suppress gene transformation by oncogene H-ras, in U94-stably expressing NIH 3T3 cell line. Ifon et al. demonstrated that the anti-cancer activity of U94 was sustainable also *in vivo* as tumor development was inhibited in nude mice treated with U94 recombinant PC3 cell line possibly due to FN 1 (Fibronectin 1) dramatic upregulation (almost 91-fold) and downregulation of ANGPTL4 levels (almost 20-fold). Increased levels of FN-1 lead to accelerated FN1-FN1 polymerization and FN1 binding to the PC3 cell surface, which could be a possible explanation at least in part, for decreased focus formation *in vitro* and tumorigenesis *in vivo*. Moreover, the expression of SPUVE 23, a serine protease, associated with increased malignant potential was found to be downregulated in the U94 recombinant PC3 cell line.

The anti-angiogenic role of U94 was explored and observed that HHV-6 infection, both in LECs and in vascular ECs, resulted in a strong inhibition of angiogenesis [7], and that this effect is entirely due to the expression of U94/*rep* by downmodulating the activation of proto-oncogene Src and its downstream signaling pathways. Our group later showed that the U94 expression induces a partial mesenchymal-to-epithelial transition and impairs cell migration, invasion, and proliferation [27]. Although the efficiency of HHV-6 infection of ECs in vitro was low, inhibition of angiogenesis was observed in 100% of cells, suggesting it could be due to the expression of a

soluble factor, conditioning the angiogenic property of the cells in culture. HHV-6A was found to induce the expression of the non-classical class I HLA-G molecule in primary human mesothelial cells as a mechanism for viral immune-escape, down modulating both innate and adaptive immunity. For this reason, the involvement of HLA-G was investigated and confirmed as soluble HLA-G also possesses an anti-angiogenic activity, inhibiting ECs ability to form capillary-like structures *in vitro*. Nonetheless, the viral infection-induced ATF3, a member of the bZIP/CREB proteins, is able to interact directly with the HLA-G promoter while stimulating the HLA-G production mediated by virus infection [60].

| Protein	Amino acids	RCMV pr127	HHV-6A RepH6	BDPV Rep1	MDPV Rep1	GPV Rep1
RCMV pr127	337					
HHV-6A RepH6	490	21				
BDPV Rep1	627	28	22			
MDPV Rep1	626	28	22	98		
GPV Rep1	627	27	22	90	89	
AAV-2 Rep78	621	24	24	47	47	46

Cleef et al., 2004 Table representing the percentage homology between different Rep proteins from several parvo-viruses highlighting the role of evolution amongst viruses of different species.

DPP4 expression

DPP4, also known as CD26, is a 110-kDa type-II transmembrane glycoprotein that can cleave a variety of substrates, including stromal cell-derived factor 1 alpha (SDF1α), eotaxin, monocyte chemotactic protein-1 (MCP-1), interleukin 2 (IL-2), and the incretin hormones like glucagon-like peptide 1 (GLP-1) and gastric inhibitory peptide (GIP), from the amino terminus of a polypeptide with proline or alanine in the second position. DPP4 is present on the surface of different cell types, but can also be found in the circulation in a soluble form (sDPP4) upon its cleavage from the cell membrane, a process called shedding. DPP4 is expressed by endothelial cells and is involved in a wide range of biological functions [61]. DPP4 has been demonstrated to be involved in inflammatory and immune responses, angiogenesis, and extracellular matrix degradation [62]. Yet, not a lot of methodologies have been explored for measuring DPP4 levels in endothelial cells. Digital imaging fluorescence microscopy has been used so far to quantify the levels of DPP4 in endothelial cells, by quantifying the mean intensity of fluorescence-based on software-generated threshold-derived cell masks (Korkmaz et al.) [63]. We, in this study, tried to analyze the expression of DPP4 on endothelial cells using flow cytometry with the aid of an anti-CD26 (BD biosciences) antibody conjugated with fluorochrome APC. Even though, a high expression was not found on cells nucleofected with ARV p17 to investigate the expression of DPP4 in the presence of ARV p17, a minor difference was observed as compared to the mock cells. It is also due to the fact that the basal expression of DPP4 is low on endothelial cells, opposite to what is found in immune cells and epithelial cells due to which an extra step of protein concentration is required, in order to measure the expression between different conditions. In our case, digital microscopy is not of much relevance since we wanted to investigate the upregulation of DPP4 in the presence of p17 protein from avian reovirus. Eventually, ELISA for anti-CD26 was used to study the same after the protein was concentrated with centrikon.

DPP4 inhibitors like teneligliptin enhance EC proliferation, reduce apoptosis and improve ER homeostasis in cardiovascular diseases, owing to their antioxidant capacity. Tenegliptin indirectly inhibits the shedding of DPP4 by downregulating MMP1, MMP2, and MMP14 gene expression via TNFα under hyperglycemic conditions which turns out to reduce the release of the soluble form of DPP4 by HUVECs [64]. Röhrborn et al. demonstrated that DPP4 is insensitive

to brefeldin A treatment not only in skeletal muscle cells but also in SMC (smooth muscle cells) and adipocytes. They suggested that MMP1, MMP2, and MMP14 play a key role in constitutive DPP4 shedding in SMC as well as under hypoxic conditions in vitro. Moreover, not a single MMP is involved in sDPP4 release, but it is rather an interplay between different shedding enzymes in a cell type-specific manner [65].
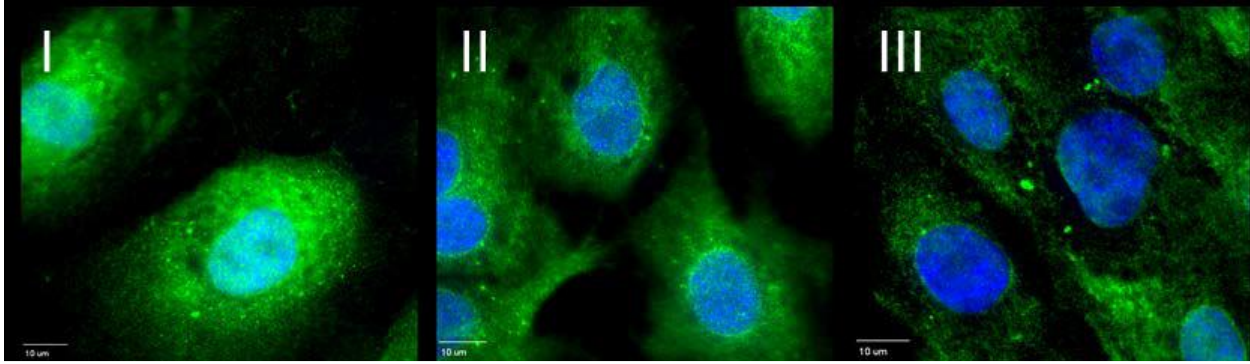
[Korkmaz et al., 2019](#) Digital microscopy analysis of DPP4 in HUVECS at different time points subjected to Homocysteine incubation.
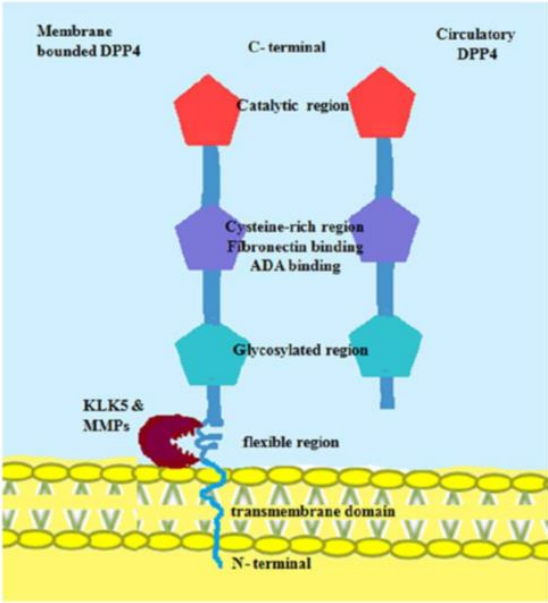
[DPP4 shedding, Chakrabarti at al., 2017](#) Schematic representation of DPP4 shedding from plasma membrane of the cells mediated by metalloproteases and other enzymes like Kallikrein-related peptidase 5.

Personal Data

In this subsection, we discuss some preliminary data obtained during the purification and optimization of dose for recombinant protein p17 from ARV used for further experiments in this study.

1. GST-ARV p17, purified after glutathione elution, was standardized primarily in MDA-MB 231 breast cancer cells for standardizing the dose range to check cytotoxicity if any, and then tested in HUVECs. No cytotoxic effects were observed for a dose range from 1 ng/ml-50 ng/ml, tested for analyzing the functional activity of protein against cell motility and invasion. The dose range of 5-20 ng/ml was found to be functional (Fig. 1) while 10 ng/ml doses being the most effective in endothelial cells and further used at the same concentration for all the biological activities. Other viral proteins like HIV p17, a structural matrix protein, are found to be present in the soluble fraction and hence is possible to extract with maximum purity and in higher amounts, using Fast Pressure Liquid Chromatography by utilizing the isoelectric point of protein elution. HIV p17 protein along with ARV p17 has been tested in some assays like tube formation assay as both the proteins are supposed to play contradictory roles in cell migration assays *in vitro* (data shown in supplementary section, Fig.S1A). However, we rule out the possibility of different methodology and constraints of purifying two different proteins from different sources affecting the final outcome on the biological activities. Moreover, the functional dose of both the protein is almost the same, which is in the range of 10-20 ng/ml and could add to the reproducibility of their respective functions. Another protein used in this study is human recombinant GST protein which has been used as a control and was used at the dose of 10nM as provided by the manufacturer. The protein was found to be non-toxic for human endothelial cells and used as 24 h pre-stimulation to the cells as per the case of ARV p17. We suppose since the protein is tagged and is relatively bigger in size approx. 43 kDa, we were unable to see the function of the protein when used as a fresh stimulant. However, a pre-stimulation of 24 h appeared to be an effective treatment with the activity sustained for up to 72 hrs in some cases.
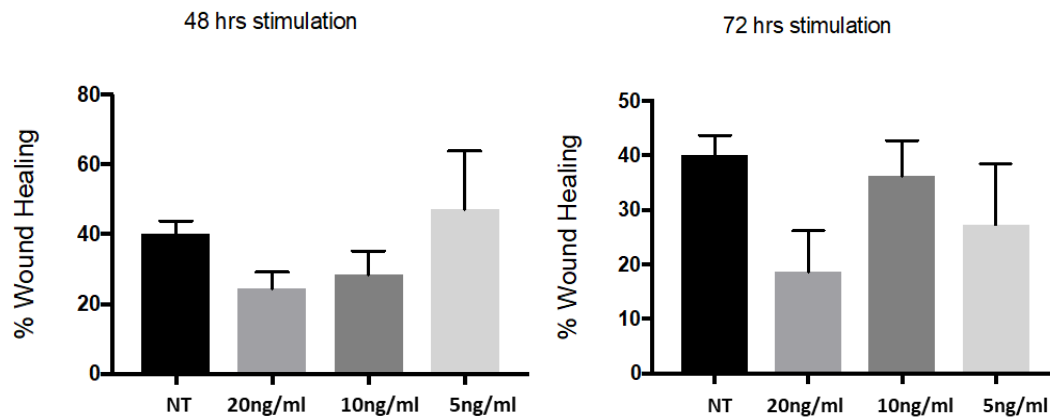
Fig.1 MDA-MB 231 cells stimulated with different concentration of ARV p17 at different time points and scratched with a manual wound to perform wound healing assay.

2. Transduced cells are processed with a nucleofection solution (Lonza) followed by a shock treatment which could affect the cell signaling and the expression of certain genes when quantified at the protein level. Cell signaling pathways like p-AKT and downstream signal p-PTEN have already been reported to be modulated in the presence of ARV p17 in cell lines like Vero and BHK. AKT and ERK are known to be the major pathways involved in cancer and angiogenesis regulation as we have also reported in our studies with HIV p17 where these pathways were upregulated in the presence of the viral protein. So, we checked for the same in the endothelial cells in the presence of ARV p17 and were able to find modulation in these pathways to a limited, but not significant extent. On the other side, p-ERK was found to have no effect when analyzed in the nucleofected cells, so we chose to check the same following protein administration with GST used as a control (data not shown). Both of the recombinant proteins, GST and GST-ARV p17 were added to the culture for 15 minutes before lysate preparation at the concentration of 10 ng/ml, while GAPDH was used as the loading control. And not a significant difference was found between GST and ARV p17 treated cell lysates, which led us to a conclusion that possibly different pathways are involved in regulating the angiogenic activity of p17 from avian reovirus in HUVECs, which remains to be investigated in future studies.

3. Endothelial cells were starved to study the effect of ARV p17 on starvation as previous studies have suggested for the viral protein to be more efficient in retarding the growth of the cells under starvation conditions in Vero, BHK, 293, and HeLa cells (Liu et al., 2005). They found that the p17-mediated effect was more clear and stronger when cells were cultured with lower serum concentrations such as 1% and 0.1%. The ARV p17 expression increased the doubling time as compared to vector-transfected cells in trypan blue viability assay, whereas in MTT assay cell growth inhibition was observed. Other viral proteins are also known to exert their activity efficiently when cells are cultured under starvation conditions [41]. In our experiments, we starved the cells overnight with 0.5% serum in endothelial basal medium (EBM). In the case of endothelial cells, no stronger effect of p17 was observed in inhibiting the cell migration in wound healing assay as compared to non-starved condition (10% FBS) (Fig. 2). Furthermore, ARV p17 was still able to suppress the tube formation activity mediated by HIV-p17 upon starvation of endothelial cells (supplementary data, S1B).
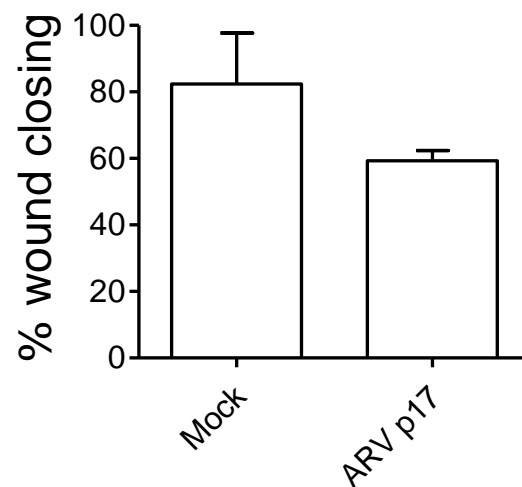

Fig. 2 HUVECs cells nucleofected with ARV p17 maintained in EBM with 0.5% FBS (starvation) and scratched with a manual wound to perform wound healing assay 48 h post nucleofection. The wound width was measured and the relative wound area was calculated as the ratio of the remaining area at 8 h time point to 0 h starting point.

3. MATERIAL AND METHODS

3.1 Cell cultures

Human umbilical vein endothelial cells (HUVECs) were isolated and characterized as previously described [66]. Cells were cultured in endothelial cell growth medium (EGMMV; Promo cell, Heidelberg, Germany) supplemented with 10% (vol/vol) Fetal Bovine Serum (FBS) at 37°C in a humidified atmosphere of 5% CO_2. Human lung microvascular endothelial cells (HMVEC-Ls) were purchased from Clonetics (San Diego, USA) and cultured in EGM-2MV (Lonza) containing 10% FBS and growth factors (EGM-MV2 BulletKit; Lonza, Basel, Switzerland). Adherent cells were cultured until 80-90% confluence. All experiments were carried out with cells at passage 2-6.

3.2 Cloning, production, and purification of recombinant GST-ARV p17

The coding sequence of ARV p17 [accession number: AAK18187.1] has been synthesized (Integrated DNA Technology, Coralville, Iowa, USA) and cloned into the XBA1 and APA1 sites of the expression vector pVAX1 plasmid (Thermo Fisher Scientific, MA, USA).

For recombinant GST-ARV p17 protein purification, the full-length ARV p17 gene was amplified from pVAX1 vector using the following primers: 5'-CGCTCGAGGGATCCATGCAATGGC-3' (forward) and 5'-GCGGGTTTAAACCTCGAGTCATAGATC-3' (reverse) (0.2 µM; Integrated DNA Technology), and cloned into the prokaryotic expression vector pGEX-4T-1 (GE Healthcare, Chicago, IL, USA) and expressed in BL21 strain of *Escherichia coli*. Selected bacterial clones were induced with 2 mM IPTG at 30° C for 3 h and GST-ARV p17 protein was recovered from the insoluble fraction of bacterial lysates, purified under denaturing conditions using 6 M urea (Sigma-Aldrich, St. Louis, MO, USA), followed by an overnight dialysis with a urea gradient in dialysis buffer (EDTA 100mM, Tris HCl 1M, DTT 1M, PMSF 100mM, 1% Triton X-100). Finally,the recombinant protein was eluted from glutathione-sepharose column (GE Healthcare) by affinity purification in elution buffer (50 mM Tris, 10mM reduced glutathione, 5mM DTT, pH 8.0). Recombinant human GST protein was obtained from Abcam (Cambridge, UK) and was used as a negative control. Visualization of protein bands was done by staining with 0.25%

Coomassie brilliant blue R-250 (Bio Rad, CA, USA) following separation on a 14% SDS-PAGE gel. The identity of the purified GST-ARV p17 protein was confirmed by western blotting as follows: Recombinant GST- and GST-ARV p17 protein were separated on a freshly prepared gel and transferred onto PVDF membrane (polyvinylidene fluoride membrane, GE Healthcare). After blocking with 3% BSA (bovine serum albumin) in Tris buffer saline containing 0.01% Tween 20 (TBS-T), the blot was probed with goat anti-GST antibody (1:2000) (GE Healthcare). The antigen–antibody complex was detected using peroxidase-conjugated donkey anti-goat IgG (Thermo Fisher Scientific) and developed using the enhanced chemiluminescence (ECL) system (Santa Cruz Biotechnology, Texas, USA).

3.3 Nucleofection

Nucleoporation of ECs was performed using the Amaxa Nucleofector Technology (Lonza) following the manufacturer's protocol. Endotoxin-free plasmid expressing ARV p17 (4 µg) was added to 1×10^6 cells resuspended in 100 µl of nucleofection buffer. Mock nucleofected cells (nucleofected with nucleofection solution only) were used as a negative control. Experiments were carried out at 48 h post nucleofection.

3.4 Cell proliferation assay

Mock- and ARV p17-nucleofected cells, were seeded in 6-well plates at a density of 1×10^6 cells/well and passaged 1:2 when they were grown to approximately 80% confluence. At the indicated time points, cells were trypsinized and counted using trypan blue exclusion.

3.5 RNA extraction, PCR and quantitative Real-Time PCR Analysis

Total RNA was extracted from HUVECs using the RNeasy Plus Mini Kit (Qiagen, Hilden, Germany) and reverse transcribed (Applied Biosystems, Foster City, CA, USA). The following primers were used to perform PCR: ARV p17 (0.2 µM; Integrated DNA Technology): 5'-GCCGGTTCGCTCTCTATTCA-3' (forward), 5'-ATGGATTGAGACCCGCCATC-3' (reverse) and β-actin: 5'-GGCACCCAGCACAATGAAG-3' (forward) and 5'-GCTGATCCACATCTGCTGG-3' (reverse).The PCR products of 146 bp and 115 bp

respectively, were analyzed on a 2% agarose gel. Quantitative Real-time PCR was performed on an ABI Prism 7500 sequence detection system with DPP4and β-actin TaqMan gene expression assays (Life Technologies, California, USA).

3.6 Wound healing assay

The wound healing assay was performed following previously described procedures with minor modifications [27]. Cells ($1x10^5$) were plated into collagen-coated 24-well plates overnight. Twenty-four h later, the monolayer was scratched using a 200 µl pipette tipand cultured in complete medium. The percentage of wound healing was evaluated during a period of 8-10h. ECs migration was recorded using a DM-IRB microscope system (Leica, Wetzlar, Germany), equipped with a CCD camera (Hitachi Ltd., Tokyo, Japan) and connected to a computer via a frame grabber (Matrox Meteor). Analysis of the images was performed using the QWin-litesoftware (Leica). In some experiments, confluent EC monolayers were pretreated, before scratching, with conditioned medium from Mock- or ARV p17-nucleofected cells for 16 h. In other experiments, EC monolayers were scratched and then cultured in the presence of 10 µM Diprotin A (DPA; Abcam).

3.7 Cell motility assay

The cell motility assay was performed as previously described [7]. Tissue-culture flasks were coated with collagen I (Sigma-Aldrich). HUVECs were added to the bottom of the coated flasks at a concentration of ~10^5 cells/flask and allowed to adhere by overnight incubation in upright position. Flasks were subsequently positioned at a ≈ 20° angle, so that both the cell-coated surface and the empty surface were immersed in culture medium. Cell motility rates were analyzed at day 10 by measuring the distance from the edge of the flask to the leading edge of the cells and photographed with a Hitachi KP-D50 camera.

3.8 Tube formation assay

Tube formation assays were performed as previously described [67]. Shortly, 150 µl of Cultrex Basement Membrane Extract (BME; 10 mg/ml) (Trevigen Inc., Gaithersburg, MD, USA) was

transferred to prechilled 48-well culture plates. Plates were then incubated for 1 h at 37º C. Cells were resuspended in EGM containing 10% FBS, seeded 5×10^4 per well and tube formation was observed during a period of 6 h after cell seeding. The capillary-like structures were photographed with a Hitachi KP-D50 camera and then quantified as number of tubes/well.

In some experiments, a co-culture between Mock- or ARV p17-nucleofected HUVECs was performed using 6-well plates with 0.4 µm pore-size transwell inserts (polycarbonate filters coated with collagen, Corning, New York, USA). Nucleofected cells (1×10^6 cells) were seeded in 2.6 ml EGM with 10% FBS in the lower compartment, while not nucleofected cells (1.5×10^5 in 1.5 ml EGM with 10% FBS) in the upper chamber. After 48 h of co-cultivation at 37º C, cells in the upper well were trypsinized and used to perform the tube formation assay. In other experiments, cells were seeded and cultured for tubes formation in the presence of 10 µM DPA.

3.9 3D matrigel assay

HUVECs (2×10^6 cells/ml) were mixed with an equal volume of BME (Trevigen Inc.) with FGF-2 (100 ng/ml) (Santa Cruz Biotechnology) or VEGF-A (100 ng/ml) (Miltenyi Biotec, Bergisch Gladbach, Germany). Each mixture was equally poured in 48-well plates (Corning), in the form of a spot in triplicates per experimental condition. After polymerization of the gel for 1 h at 37º C, each spot of cells embedded in Matrigel was bathed in 500µl of complete medium. After 24 h incubation, the tube formation was observed and the number of closed areas was counted. Images were captured with a Hitachi KP-D50 camera.

3.10 Spheroids assay

Spheroids were generated by mixing ECs (1×10^5 cells/ml) with 5 mg/ml of methylcellulose (Sigma-Aldrich) in EGM medium containing 10% FBS, making the final volume to 10 ml. The cells (100 µl/well) were then added to 96-well plates (Greiner Bio-one, Kremsmünster, Austria) and incubated at 37º C, 5% CO_2 for 24 h.

Separately, the collagen I gel solution (Rat tail, Corning) was maintained on ice and neutralized by adding NaOH 0.1N and PBS 10X to a final pH of 7.4. Then, the 24-well plates were coated with neutralized collagen (200µl/well) and incubated in a humidified 5% CO_2 incubator for 1 h at 37º C. The spheroids from 96-well plates were collected in eppendorf tubes and centrifuged at

2000Xg for 5-10 sec. When a clear pellet was distinguished, the supernatant was removed and the pellet was kept in a volume of about 50 µl collagen I-neutralized solution. Each collagen-spheroid mixture was rapidly added to the precoated 24-well plates at 50 µl/well and incubated for 1 h. After 1 h, 500 µl of conditions (FGF-2 at 100 ng/ml or VEGF-A at 30 ng/ml or DPA at 10µM) were added to the wells to cover the surface completely and plates were further incubated for 24 h. Sprouting occurred from the spheroid core, photographed with a Hitachi KP-D50 camera, and the sprout number (mean ± SD) was counted with the spheroids of similar sizes from three different wells of the plate.

3.11 Immunofluorescence

Cells treated with GST- or GST-ARV p17 were fixed, permeabilized, blocked with 0.1% BSA and incubated overnight with a rabbit polyclonal antibody to ARV p17 (dilution of 1:100; Abcam). Then, cells were washed and incubated with AlexaFluor 488 conjugated secondary antibody goat anti-rabbit IgG (dilution of 1:500; Thermo Fisher Scientific) for 1 h at room temperature. After three washes with PBS, slides were mounted and samples were observed using a Leica (Wetzlar, Germany) TCS SP5 laser scanning fluorescence microscope and the imaging software Leica Application Suite.

3.12 Aortic Ring Assay

The assay was performed as previously described [68]. Aortic rings obtained by cross-sectioning the thoracic aorta of 2-month-old C57BL/6 female mice were incubated in serum-free medium in the presence of recombinant GST- or GST-ARV p17 (10 ng/ml). After 24 h, rings were embedded in fibrin gel and incubated with serum-free endothelial cell basal medium (EBM, Clonetics) plus 10 µg/ml aprotinin in the absence or presence of FGF-2 (100 ng/ml). Medium and stimuli were replaced every day. After 6 days, vessel sprouts, morphologically distinguishable from scattering fibroblasts/smooth muscle cells, were counted under a stereomicroscope (STEMI-SR, Zeiss).

3.13 Chick Chorioallantoic Membrane (CAM) assay

Alginate beads (4.0 µl) containing vehicle or 100 ng of FGF-2 with or without GST- or GST-ARV p17 (both at 20 ng/pellet) were prepared as previously described [69] and placed on the top of the embryo CAM of fertilized White Leghorn chicken eggs at day 11 of incubation. After 72 h, newly formed blood microvessels converging towards the implant were counted in ovo at 5× magnification under a stereomicroscope (STEMI-SR, Zeiss, Oberkochen, Germany).

3.14 Angiogenesis Microarray Analysis

HUVECs were nucleofected and cultured for 24 h, then conditioned medium was collected, clarified and analyzed for the expression of 55 different angiogenesis-related proteins by Human Angiogenesis Array Kit (Proteome Profiler, R&D systems, Minneapolis, USA) according to the manufacturer's instructions.

3.15 Human DPP-4/CD26 ELISA

HUVECs were stimulated with GST- or GST-ARV p17 for 48 h, and then conditioned medium was collected, clarified and concentrated with Centricon Amicon YM-30 (cut off 30 kDa). The release of DPP4 in the concentrated conditioned medium was evaluated using human CD26 ELISA Kit (R&D systems) according to manufacturer's instructions. Each sample was analyzed in triplicates.

Statistical analysis

Data obtained from multiple independent experiments are expressed as the means ± the standard deviation (SD). The data were analyzed for statistical significance using Student's t-test or one-way ANOVA. Bonferroni's post-test was used to compare data. Differences were considered significant at $P < 0.05$. Statistical tests were performed using Prism 8 software (GraphPad, San Diego, CA, USA).

4. RESULTS

4.1 Wound healing assay on different nucleofected cell lines

Growth retardation effects of ARV p17 has been reported before in several studies on multiple normal and cancer cell lines like Vero, HeLa, BHK, HEK 293 and A549 cells. To replicate the growth inhibiting effects of ARV p17 on cancer cell line like HeLa, which has already been reported via transfection, nucleofection was performed on HeLa to check the toxicity, if any, upon ARV p17 expression and assess the cell viability. As shown in Fig. 3A, the cell viability was not affected upon administration of the viral protein and was not toxic to the cultured cells, even though a slight insignificant dip in the growth of the ARV p17-nucleofected cells was observed as compared to mock-nucleofected cells. Followed by which, cell migration assay was performed with cell motility assay and wound healing assay post 48 h of nucleofection. Cell migration was inhibited by almost 50% in the presence of ARV p17 Fig. 3(B, C). Human fibroblasts were also used to test the efficacy of ARVp17 on wound healing assay by nucleofection (Fig. 4). Like HeLa, cell migration was also inhibited in fibroblast cells by ARV p17 expression up to a similar extent. These results signify that not just on cell cycle and cell growth but the viral protein also exerts anti migratory effects despite of the origin of cell line, upon endogenous mode of administration.
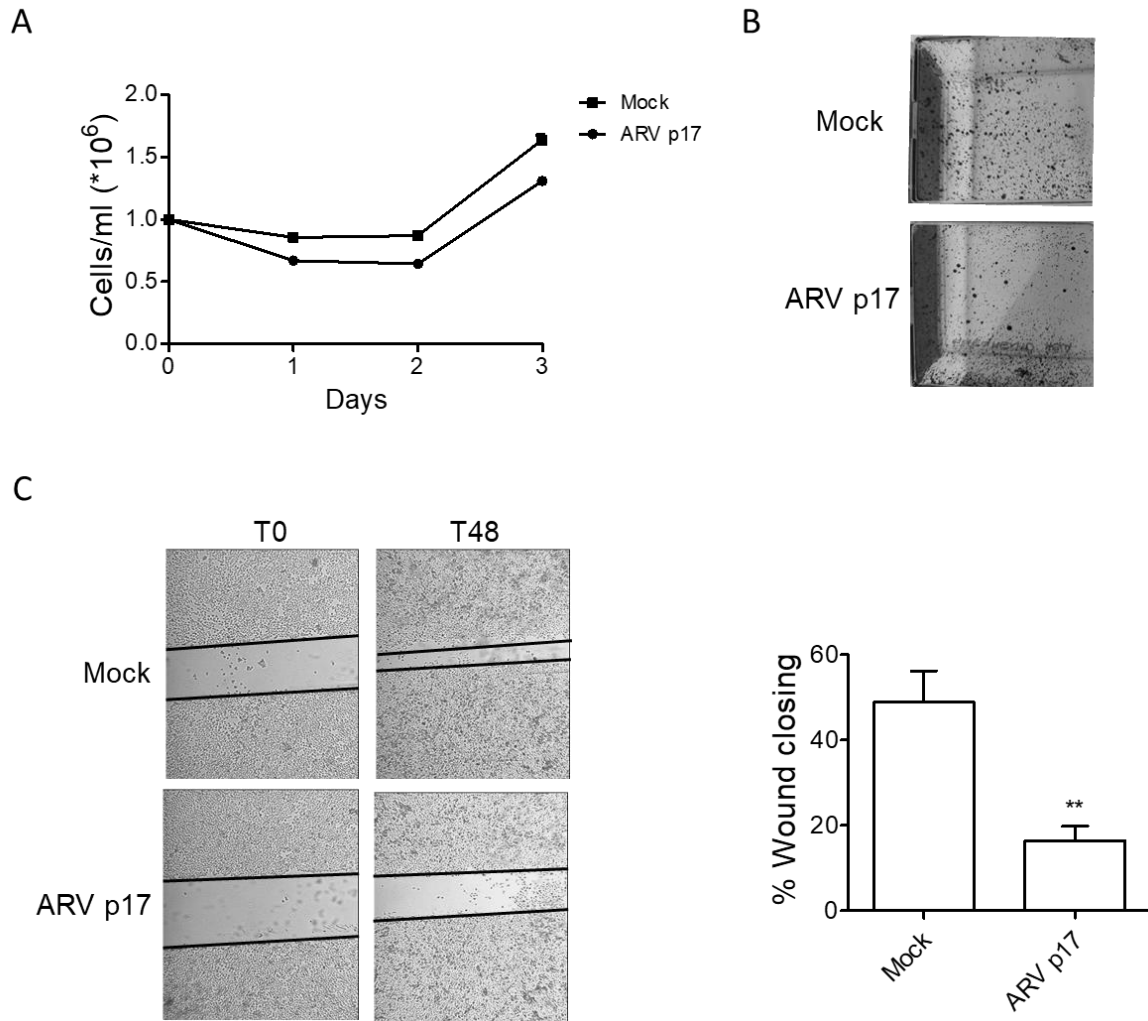
Fig. 3 **ARV p17 expression inhibits HeLa cells migration** (A) HeLa cells were mock-nucleofected (Mock) or nucleofected with ARV p17-expressing plasmid (ARV p17). At each time point, cells were counted using the trypan blue exclusion method. Values represent the mean ± SD of one representative experiment out of three with similar results, performed in triplicates. (B) Cell movement along the bottom of an angled flask was recorded at day 8 post nucleofection. (C) HeLa cells nucleofected with ARVp17 and scratched with a manual wound to perform wound healing assay 48h post nucleofection. The wound width was measured and the relative wound area was calculated as the ratio of the remaining area at 48 h time point to 0 h starting point.
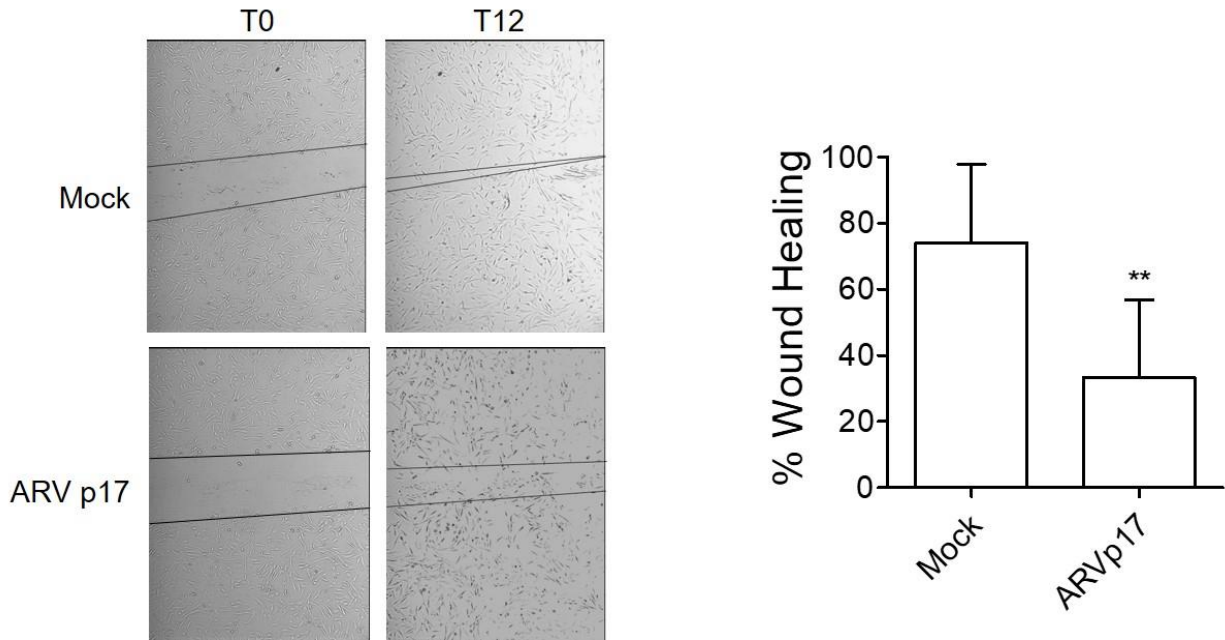
Fig. 4 **ARV p17 expression inhibits fibroblasts migration** Fibroblast cells nucleofected with ARVp17 and scratched with a manual wound to perform wound healing assay 48h post nucleofection. The wound width was measured and the relative wound area was calculated as the ratio of the remaining area at 12 h time point to 0 h starting point.

4.2 Effect of ARV p17 on breast cancer cells

Since ARVp17 has been reported to suppress carcinogenesis in multiple cell lines, we started off to check the activity of recombinantly purified ARV p17 in MDA-MB 231 breast cancer cell line. As shown in Fig. 5A, wound healing assay performed 48 h post treatment with ARV p17, inhibited the migration of the cells to more than 50% as compared to the GST treated cells. In order to understand the secretion of any factors in the conditioned medium related to the anti-carcinogenic activity of the protein, we performed an oncogenic array from the secretome of MDA-MB 231 cells.

As indicated in Fig. 5B, levels of cell cycle regulatory factors, like p27 and p53 were found to be upregulated in CM from ARV p17 nucleofected cells. On the other hand, anti-carcinogenic factor like endostatin was upregulated almost 4 times more than mock cells. At the same time, some of the carcinogenic factors like CEACAM-5 and thrombospondin-1 were downregulated in ARV p17 expressing cells, testifying for the cancer modulating activity of ARV p17 in breast cancer by the mode of secretion of anti-carcinogenic factors in the conditioned medium.
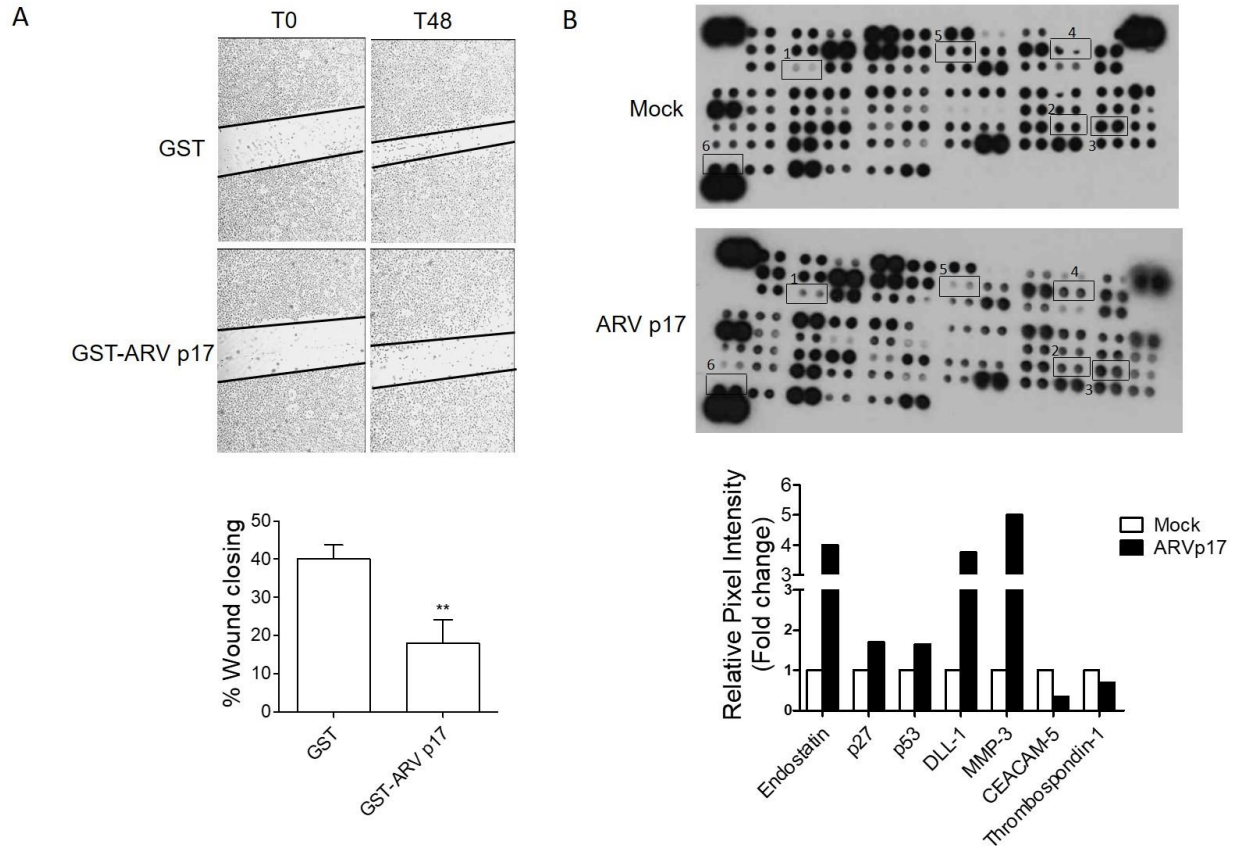
Fig. 5 **Effect of ARV p17 on breast cancer cells** (A) MDA-MB 231 cells stimulated with recombinant GST-ARVp17 for 48h and scratched with a manual wound to perform wound healing assay. (B) Oncogenic array with supernatant from MDA-MB 231 cells nucleofected with Mock or ARV p17. Relative pixel intensity was calculated using ImageJ software and expressed as the mean of duplicate dots.

4.3 ARV p17 expression in nucleofected cells

HUVECs were nucleofected with the nucleofection solution alone (Mock) or with the plasmid vector pVAX expressing ARV p17 (ARV p17). To ensure that the nucleofected sequences were functional, cells harvested at different time points post nucleofection were analyzed for the presence of ARV p17 mRNA by RT-PCR analysis (Figure 6A). ARV p17 transcripts were detected at day 2 post nucleofection, whereas a weak or faint expression was evident at day 4 and day 6, respectively. Moreover, cell proliferation was followed every 2 days, from day 2 until day 6, and no toxic effect was observed in ARV p17-expressingcells. Indeed, as shown in Figure 6B, ARV p17-expressing ECs maintained a doubling time similar to Mock HUVECs, indicating that the viral protein does not modify the cell cycle. Based on this data, all the following assays were performed at day 2 post nucleofection.
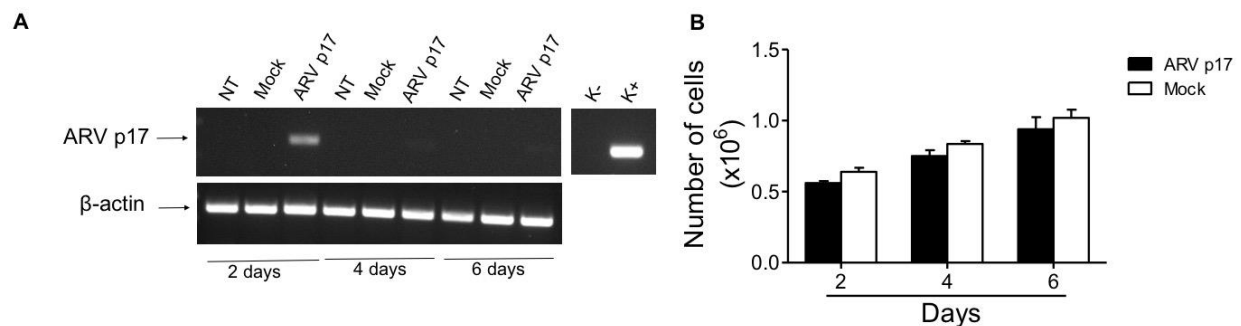
Fig. 6 **ARV p17 expression in HUVECs** HUVEC cells were mock-nucleofected (Mock) or nucleofected with ARV p17-expressing plasmid (ARV p17). (**A**) The presence of ARV p17 mRNA was analyzed by RT-PCR at different days post nucleofection. K⁻, negative control, water; K⁺, positive control, ARV p17-expressing plasmid. As a control, amplification of β-actin mRNA is also shown. (**B**) At each time point, cells were counted using the trypan blue exclusion method. Values represent the mean ± SD of three independent experiments performed in triplicates.

4.4 ARV p17 expression inhibits ECs motility and migration

The capability of ARV p17 to interfere with the migratory activity of ECs was assessed by wound healing assay. HUVECs confluent monolayers were scratched with a 200 µl tip, and the percentage of wound sealing was observed over a period of 8 h. Mock cells reached 100% of sealing 8 h after the wound while ARV p17-expressing cells, at the same time, reached 53% of sealing only (53 ± 6.1%) showing a significant inhibition in wound repair ability (Figure 7A). Then, to evaluate the effect of ARV p17 expression on long term migration of ECs, we performed an angled flask migration assay. Cell movement along the bottom of an angled flask was recorded at day10post nucleofection. Cell migration strongly decreased in ARV p17-expressing cells as compared to Mock cells, attesting for a long-standing anti-migratory efficacy of the viral protein (inhibition: 48 ± 2%) (Figure 7B). Taken together, these data highlight the ability of ARV p17 to inhibit HUVECs migration and motility.
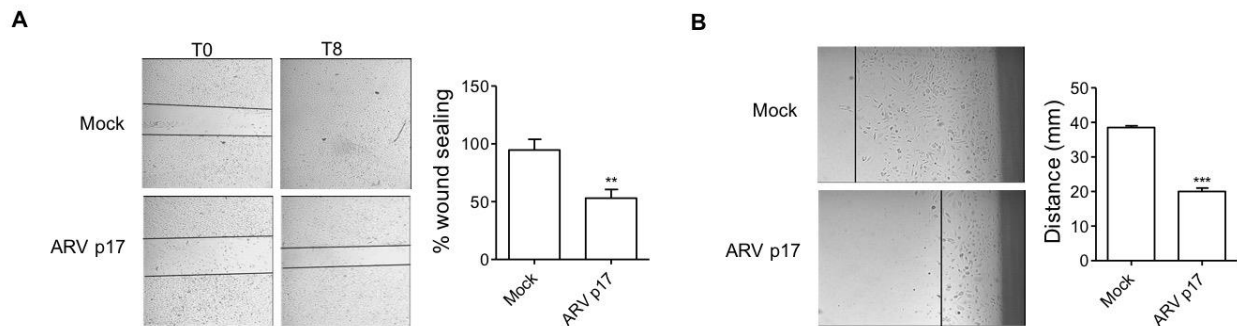

Fig. 7 **ARV p17 inhibits HUVEC cell migration** HUVEC cells were mock-nucleofected (Mock) or nucleofected with ARV p17-expressing plasmid (ARV p17). (**A**) ECs wound repair ability was analyzed 48 h post nucleofection. Confluent cell monolayers were scratched using a 200 µl pipette tip and cell migration was recorded by light microscopy for 8 h after wound scratch (original magnification, 4x). The wound width was measured and the relative wound area was calculated as the ratio of the remaining area at 8h time point to 0h starting point. (**B**) Cell movement along the bottom of an angled flask was recorded at day 10 post nucleofection (original magnification, 10x). Cell motility rate was analyzed by measuring the distance from the edge of the flask to the leading edge of the cells. Images are representative of one out of three independent experiments with similar results. Values are the mean ± SD of one representative experiment out of three with similar results, performed in triplicates. Statistical analysis was performed by Student's t test. ** $P < 0.01$; *** $P < 0.001$.

4.5 ARV p17 expression inhibits angiogenesis

The ability of ARV p17 to regulate the angiogenesis of ECs was investigated by *in vitro* tube formation assay. Cells were seeded on 48-well plates (5×10^4/well) containing polymerized plugs of basement membrane extract (Cultrex). As shown in Figure 8A, Mock HUVECs formed a consistent network of capillary-like structures (61±3), whereas ARV p17-expressing cells seeded and cultured ≤6 h on Cultrex BME, lost the ability to form tubes almost completely (39 ±6).

Next, tube formation assay was studied using a 3-dimensional (3D) Matrigel culture. Mock and ARV p17 ECs were mixed with Matrigel and FGF-2 (Fibroblast Growth factor 2; 100 ng/ml), and as shown in figure 8B, within 24 h of incubation, activated cells migrated and aligned to form tubes organized in a capillary-like network (70 ± 8). Interestingly, ARV p17-expressing cells significantly reduced the mean of the number of closed areas lined by the tubes by a great margin (18± 2). The entrapment of EC spheroids in biopolymeric gels, is based on the property of ECs to form spheroids under non adherent conditions, and represents a 3D cell model that mimics *in vivo* sprouting angiogenesis [70]. Mock and ARV p17 HUVEC-derived spheroids were treated with FGF-2, and a 3D organotypic culture was performed. As shown in Figure 8C, as expected, stimulation of spheroids with FGF-2 strongly promoted microvessels outgrowth (39 ±3). Interestingly, ARV p17 induced a dramatic reduction of sprouts outgrowth in HUVEC spheroids in 24 h (4 ± 3). These data strongly suggest that even in a 3D environment, ARV p17 displays a potent anti-angiogenic activity. Moreover, ARV p17 in addition to interfering with mechanisms underlying spontaneous angiogenesis also renders cells insensitive to the potent FGF-2-induced vasculogenetic activity.
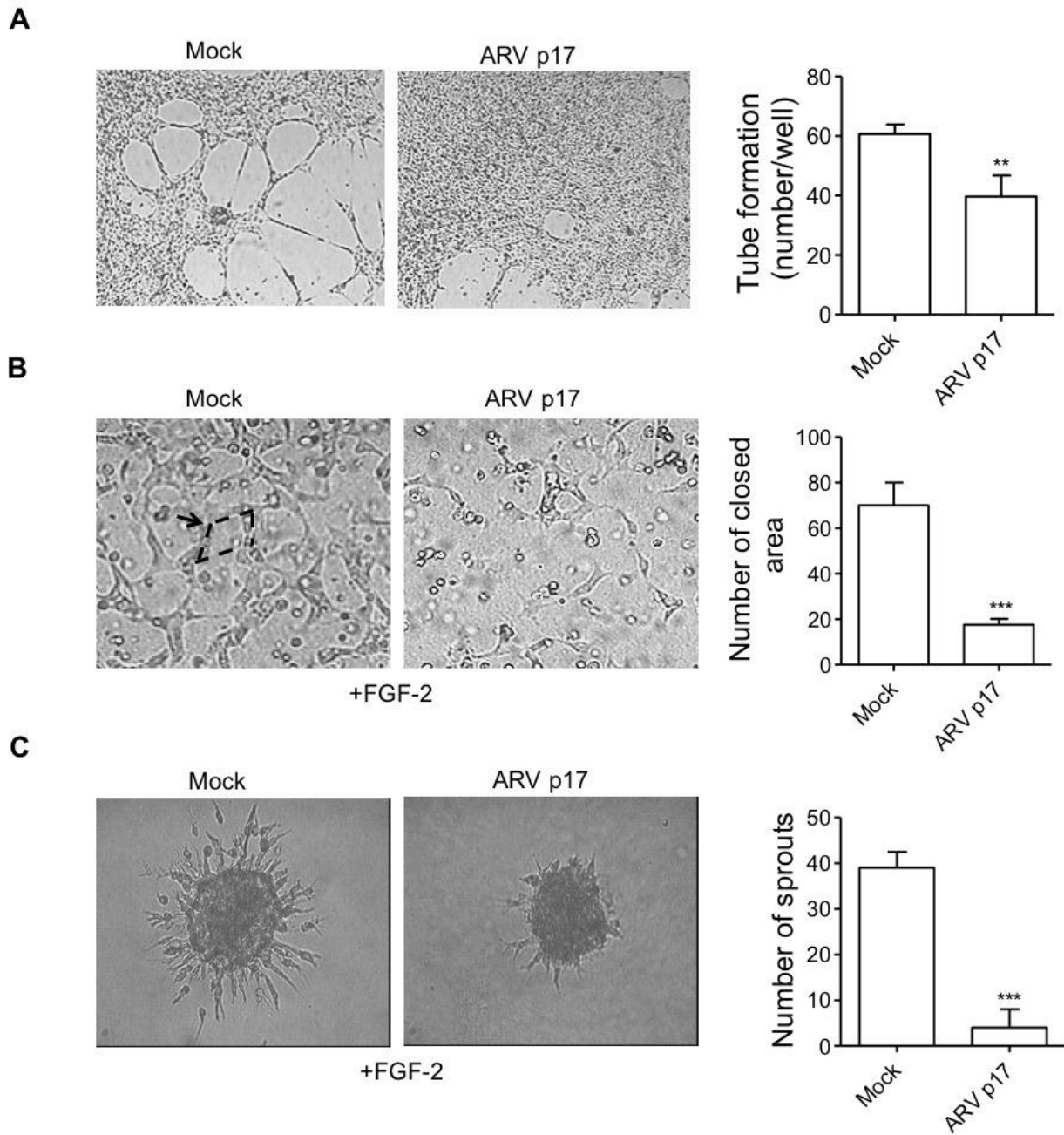
Fig. 8 **ARV p17 inhibits ECs angiogenesis** HUVEC cells were mock-nucleofected (Mock) or nucleofected with ARV p17-expressing plasmid (ARV p17). Angiogenesis was analyzed 48 h post-nucleofection. (**A**) HUVECs were seeded on BME-coated plates. Images were taken after 6 h of HUVEC culture on BME (original magnification, 4x). Closed rings were counted as a parameter for quantification of tube formation. (**B**) Tube formation of Mock or ARV p17 HUVECs along with FGF-2 treatment in a 3D Matrigel culture. Lined by the tubes, the closed areas (an example indicated by the arrow) were counted as a parameter for quantification of tube formation. Pictures were taken after 24 h of culture (original magnification, 10×). (**C**) Sprouting of spheroids generated by Mock or ARV p17 HUVECs upon FGF-2 treatment. Pictures were taken after 24 h of culture (original magnification, 20×). The bar graph shows the average number/spheroid of EC sprouts. Pictures are representative of one out of three independent experiments with similar results. Values are the mean ± SD of one representative experiment out of three with

similar results, performed in triplicates. Statistical analysis was performed by Student's t test. ** P < 0.01; *** P < 0.001

4.6 Recombinant GST-ARV p17 production and expression

We produced and purified the recombinant ARV p17 protein with a GST tag at the N-terminus (GST-ARV p17) and, as expected, a band of 43 kDa was observed in a Coomassie stained gel (Figure 9A). The identity of the protein was confirmed by western blot analysis using a goat anti-GST antibody (Figure 9B). Previous findings, obtained by transfection of epithelial cells, demonstrated that ARV p17 is a nucleocytoplasmic shuttling protein [16]. Based on this knowledge, we performed immunofluorescence analysis to evaluate the ability of GST-ARV p17, administered exogenously, to enter inside endothelial cells. To this aim, HUVECs were treated for 16 h with 10 ng/ml of GST-ARV p17 protein and cells treated with recombinant GST were used as a negative control. The localization of the viral protein has been revealed by using a polyclonal antibody to a synthetic peptide derived from the ARV p17. As shown in Figure 9C, within 16 h of treatment, ARV p17 internalizes in ECs as displayed by the bright punctate staining in the cell cytoplasm. As expected, GST-treated ECs, used as a negative control, showed no positive staining.
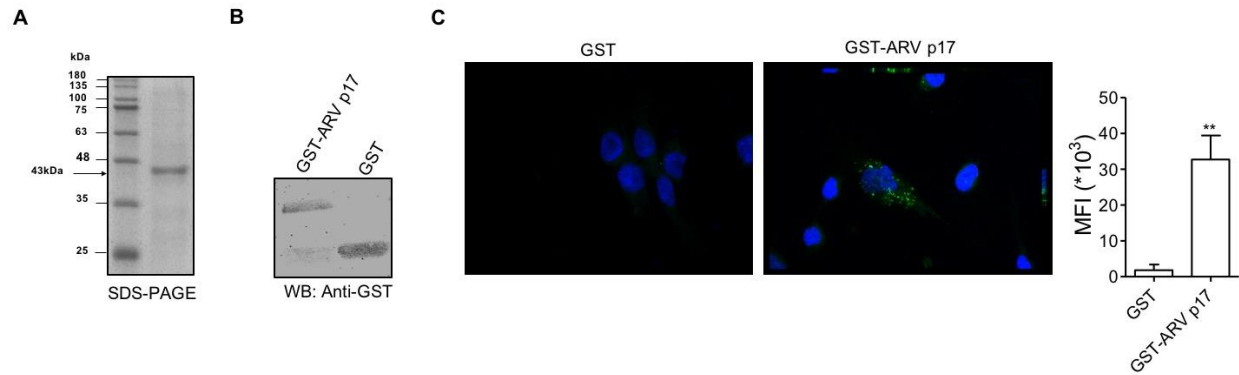
Fig. 9 **Recombinant GST-ARV p17 characterization** (**A**) Purified recombinant GST-ARV p17 protein analyzed by SDS-PAGE electrophoresis and stained with Coomassie. (**B**) Western blot analysis of recombinant GST and GST-ARV p17by goat anti-GST antibody. (**C**) HUVECs were treated for 16h at 37°C with 10ng/ml of recombinant GST or GST-ARV p17. Images display GST-ARV p17 signals in green and cell nuclei in blue. Bar graph displays mean fluorescence intensity observed for ARV p17 signal quantification. Pictures are representative of five selected fields/sample (original magnification, 63×). MFI = Mean Fluorescence Intensity. Statistical analysis was performed by Student's t test. ** P < 0.01.

4.7 Exogenous ARV p17 suppresses EC migration and angiogenesis

We performed experiments to determine if the recombinant GST-ARV p17 protein, added exogenously to ECs cultures, induces the same activity observed after nucleofection of the ARV p17 gene. To this end, HUVECs were pretreated with GST-ARV p17 (10 ng/ml) for 24 h whereas GST protein was used as a negative control.

We studied the effect of GST-ARV p17 on *in vitro* wound healing drawn via mechanical injury. HUVECs confluent monolayers were scratched with a 200 µl tip and the percentage of wound sealing was observed over a period of 8 h. As shown in Figure 10A, control HUVECs, treated with the GST protein, reached 96±6% of sealing, whereas GST-ARV p17-treated HUVECs reached only 56± 3% of sealing, showing a considerable inhibition in scrape wound repair ability.

HUVECs treated with GST-ARV p17weretransferred on BME-coated plates, and observed for the formation of capillary-like structures. As shown in Figure 10B, the number of tubes produced by GST-ARV p17-treated ECs resulted in the formation of a fewer capillary-like structures (30±4) when compared to GST-treated cells (56 ±6).

To assess whether exogenously administered GST-ARV p17 is able to counteract the activity of a well-known pro-angiogenic factor such as FGF-2, we performed 3D matrigel assay in the presence of FGF-2 (100 ng/ml). As shown in Figure 10C, within 24 h of incubation, GST pretreated cells formed a capillary-like network upon FGF-2 stimulation (47 ± 2). On the contrary, pretreatment of GST-ARV p17 drastically reduced the number of closed areas on addition of FGF-2 (3 ±2). Similar results were obtained by FGF-2stimulated spheroids.

Indeed, as shown in Figure 10D, stimulation of GST-derived spheroids with 100 ng/ml of FGF-2, as expected, strongly increased the outgrowth of sprouts (28±2). On the other hand, FGF-2 angiogenic activity was completely abolished by GST-ARV p17 (12±1).

Taken together, these data demonstrate that ARV p17 induces remarkable anti-migratory and anti-angiogenic activity by both endogenous and exogenous administration. In a similar manner, ARV p17 is also able to strongly suppress the activity of a potent pro-angiogenic molecule. To our knowledge, this is the first study showing the effect of recombinantly purified p17 protein from avian reovirus to mediate biological activities relative to nucleofection.
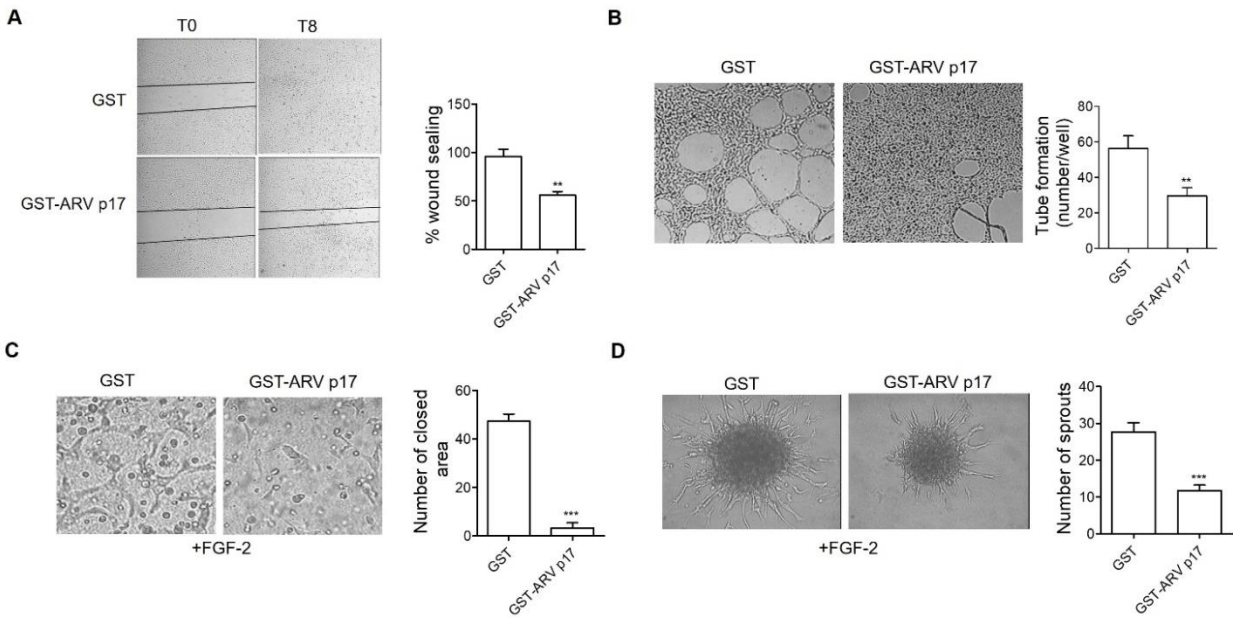
Fig. 10 **Effect of recombinant GST-ARV p17 protein on angiogenesis** HUVECs were pretreated with10 ng/ml of either recombinant GST or GST-ARV p17 for 24 h. (**A**) Wound healing assay to assess migratory activity of ECs. Confluent cell monolayers were scratched using a 200 μl pipette tip and cell migration was recorded by light microscopy 8 h after wound scratch (original magnification, 4x). The wound width was measured and the relative wound area was calculated as the ratio of the remaining area at 8 h time point to 0 h starting point. (**B**) Matrigel assay to assess tube formation activity in GST- and GST-ARV p17-pretreated cells. Pictures were taken after 6 h of culture (original magnification, 4×). Closed rings were counted as a parameter for quantification of tube formation. (**C**) 3D matrigel assay in the presence of FGF-2 (100 ng/ml) to assess the tube formation in GST- and GST-ARV p17 pretreated cells. Pictures were taken after 24 h from cell seeding (original magnification, 10×). The closed areas were counted as a parameter for quantification of tube formation. (**D**) Spheroid assay in the presence of FGF-2 (100 ng/ml) to assess sprout formation in GST- and GST-ARV p17 pretreated cells after 24 h (original magnification, 20×). The bar graph shows the average number/spheroid of EC sprouts. Pictures are representative of one out of three independent experiments with similar results. Values are the mean ± SD of one representative experiment out of three with similar results, performed in triplicates. Statistical analysis was performed by Student's t test. ** $P < 0.01$; *** $P < 0.001$.

4.8 ARV p17 protein suppresses the activity of different angiogenic molecules

The evidence that ARV p17 strongly suppresses the anti-angiogenic activity of FGF-2, prompted us to further scrutinize this aspect with another well-known pro-angiogenic factor. To this end, we performed key experiments upon Vascular Endothelial Growth Factor A (VEGF-A) stimulation. HUVECs were pretreated with either protein, as described above, and then plated for 3D Matrigel culture. Mock and ARV p17 ECs were mixed with Matrigel and VEGF-A (100 ng/ml). Interestingly, as shown in Figure 11A, GST pretreated cells formed a capillary-like network upon VEGF-A stimulation (43±3). On the contrary, pretreatment of GST-ARV p17 considerably reduced the number of closed areas on addition of VEGF-A (10 ± 2). Similarly, stimulation of GST-derived spheroids with 30 ng/ml of VEGF-A, as expected, markedly increased the outgrowth of sprouts (32 ± 1), whereas VEGF-A angiogenic activity was significantly blocked by GST-ARV p17 (17 ±2) (Figure 11B). These data highlight the strong ability of ARV p17 to contrast different potent proangiogenic stimuli.
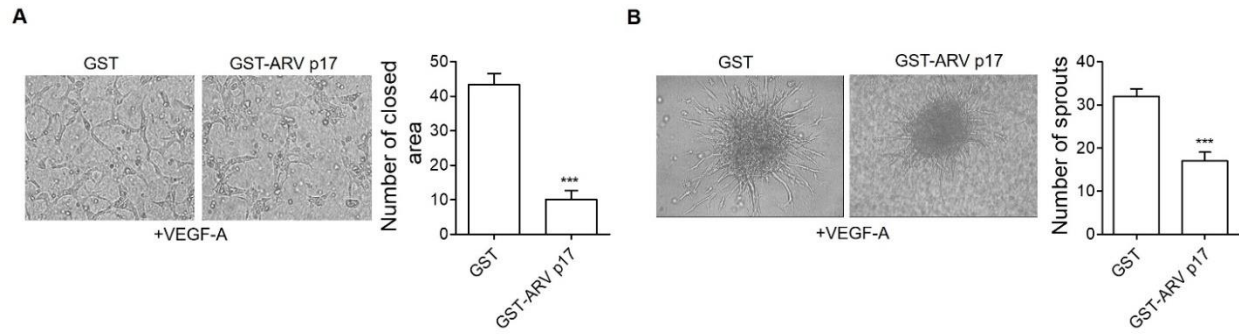
Fig. 11 **Effect of ARV p17 on VEGF-A-mediated angiogenesis.** HUVECs were pretreated with10 ng/ml of either recombinant GST or GST-ARV p17 for 24 h. (**A**) Matrigel assay in the presence of VEGF-A (100 ng/ml) to assess the tube formation in GST- and GST-ARV p17 pretreated cells. Pictures were taken after 24 h of culture (original magnification, 10×). The closed areas were counted as a parameter for quantification of tube formation. (**B**) Spheroid assay in the presence of VEGF-A (30 ng/ml) to assess sprout formation after 24 h in GST- and GST-ARV p17 pretreated cells (original magnification, 20×). The bar graph shows the average number/spheroid of EC sprouts. Pictures are representative of one out of two independent experiments with similar results. Values are the mean ± SD of one representative experiment out of two independent experiments, performed in triplicates. Statistical analysis was performed by Student's t test. *** $P < 0.001$.

4.9 ARV p17 inhibits vasculogenesis ex vivo and in vivo

The recombinantGST-ARV p17 protein was then tested for its capability to promote neovessels formation by *ex vivo* and *in vivo* experiments. To this aim, the effect of ARV p17 on angiogenesis was studied using the aortic ring assay, which allows to investigate the capability of molecules to interfere with the *ex vivo* growth of microvessels. Aortic rings were treated with GST- or GST-ARV p17 for 24 h, and then cultured in the presence of FGF-2 (100ng/ml) for 6 days. As expected, stimulation of aortic rings with FGF-2 strongly increased microvessels outgrowth (39 ± 14), as compared to NT (3±3). Interestingly, pretreatment of rings by GST-ARV p17 suppressed the number of microvessels induced by FGF-2 to a great extent (7 ± 6), but not the pretreatment by GST (33± 11) (Figure 12A). The vasculogenic property of GST-ARV p17 was furthermore investigated *in vivo* by using the chick chorioallantoic membrane (CAM) assay. As shown in Figure 12B, a significant angiogenic response in the form of numerous allantoic neovessels developing radially toward the implant in a "spoke-wheel" was promoted by 100 ng of FGF-2 (mean number of vessels: 50 ± 3) as compared to NT (mean number of vessels: 9 ± 3). As expected, GST treatment was irrelevant to FGF-2-induced vessel formation (mean number of vessels: 53± 9), whereas GST-ARV p17 treatment strongly diminished neovessels development (mean number of vessels: 22 ± 3)

These results further attest for the ability of ARV p17 to interfere with mechanisms underlying induced angiogenesis, both *ex vivo* and *in vivo*.
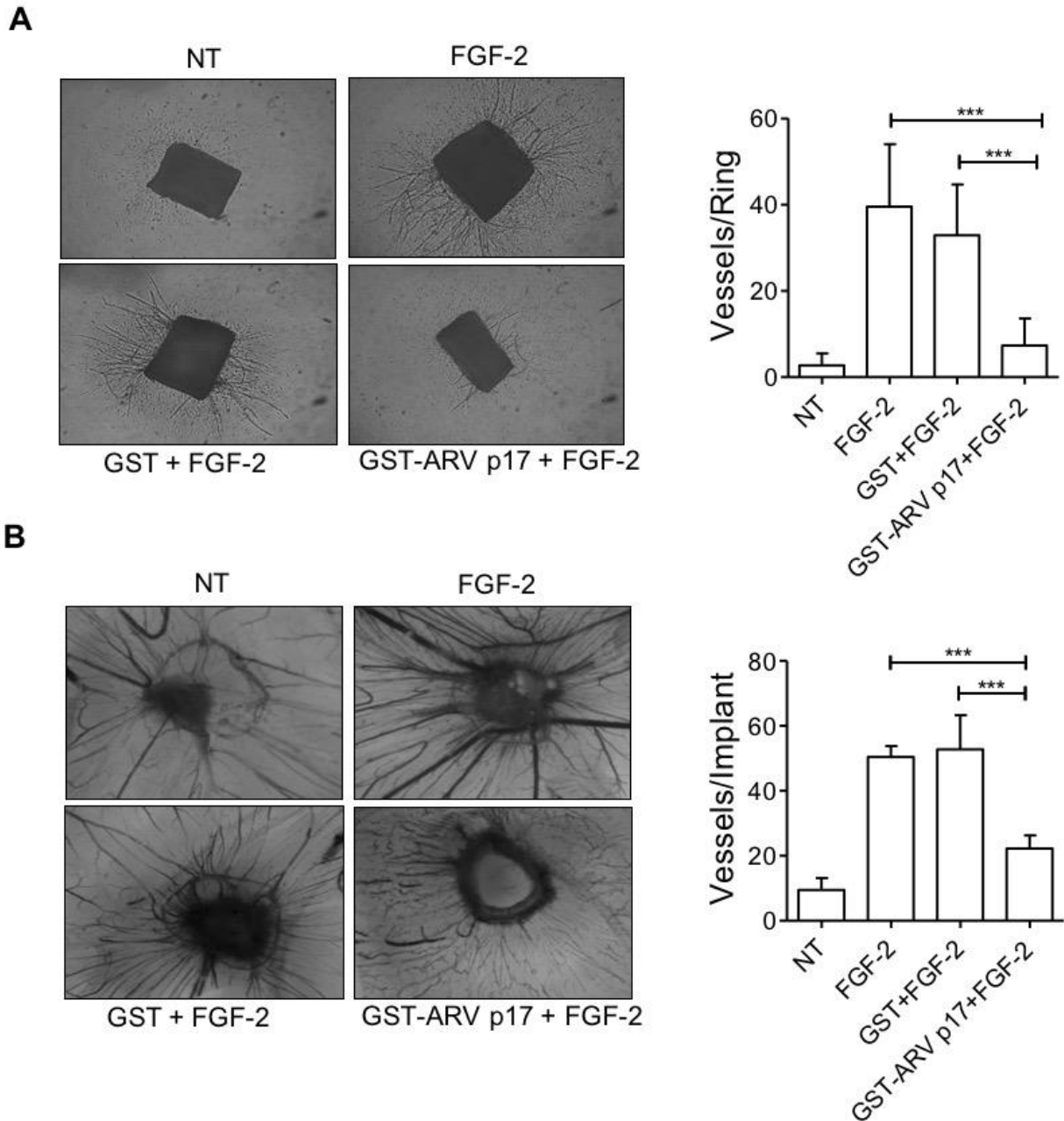
Fig. 12 *In vivo* **and** *ex vivo* **effects of ARV p17 on vasculogenic process** (**A**) Mouse aortic rings, embedded in fibrin gel, were incubated for 24 h as indicated. After 6 days, microvessels were observed, counted under a stereomicroscope and data were expressed as the number of sprouts per aortic ring (mean ± SD of 7-10 rings per experimental point). Pictures are representative of two independent experiments with similar results (original magnification, 4×). (**B**) Microvessels converging towards the implant were counted at day 14 under a stereomicroscope. Pictures of CAMs are representative of two independent experiments with similar results (original magnification, 5×). Bars represent the mean ± SD of 4-5 eggs per experimental point in two independent experiments. Statistical analysis was performed by one-way ANOVA and Bonferroni's post-test was used to compare data. *** P < 0.001.

4.10 ARV p17 influence the microenvironment through the release of an anti-antiangiogenic factor

Our data demonstrated that ARV p17 treatment interferes with the potent VEGF-A and FGF-2-inducedvasculogenetic activity leading to hypothesize that the viral protein promotes a microenvironment unfavorable to neovessel formation. To test this hypothesis, we investigated the effect of ARV p17 conditioned culture medium on the angiogenic activity of ECs. As shown in Figure 13A, pretreatment with conditioned medium obtained from ARV p17-expressing ECs on HUVECs monolayers impaired sealing of the wound ($32 \pm 2\%$), whereas this did not occur in HUVECs pretreated with medium obtained from Mock ECs ($73\pm1\%$).

Moreover, HUVECs co-cultured for 48 h in the collagen-coated upper insert well of a 0.4 μm pore-size transwell with ARV p17 expressing cells in the lower chamber, lost their ability to form tube-like structures when detached and seeded on Matrigel ($9 \pm1\%$) (Figure 13B). On the contrary, HUVECs co-cultured with Mock cells were capable of exerting angiogenesis, forming a consistent network of tube-like structures ($88 \pm 2\%$). To understand whether the anti-angiogenic activity of ARV p17was direct or mediated by other molecules, we performed analysis of ARV p17-expressing HUVEC secretome by using a human angiogenesis array. Significant results are shown in Figure 13C, ARV p17 was found to trigger the secretion of Dipetidyl peptidase 4 (DPP4) powerfully, whereas it proved unable to induce secretion of any other anti-angiogenic factors tested. Interestingly, the viral protein completely abolished the release of the angiogenic PLGF1 (Placental growth factor 1).

Increased level of DPP4 protein secretion induced by ARV p17treatment was paralleled by an increase in specific DPP4 mRNA expression. When DPP4 messages were quantified by real-time polymerase chain reaction Taqman Assay in HUVECs-expressing ARV p17 or not, we observed that DPP4 mRNA in ARV p17-nucleofectedECswas expressed at higher level (approximately 1.7-fold), as compared to Mock cells (Figure 13D). To confirm the capability of ARV p17 to promote DPP4 release by HUVECs, quantity of soluble DPP4 (sDPP4) upon GST-ARV p17 treatment was analyzed by ELISA. As shown in Figure 14E, ARV p17 induced a significant increase (approximately 7-fold) of DPP4 release.
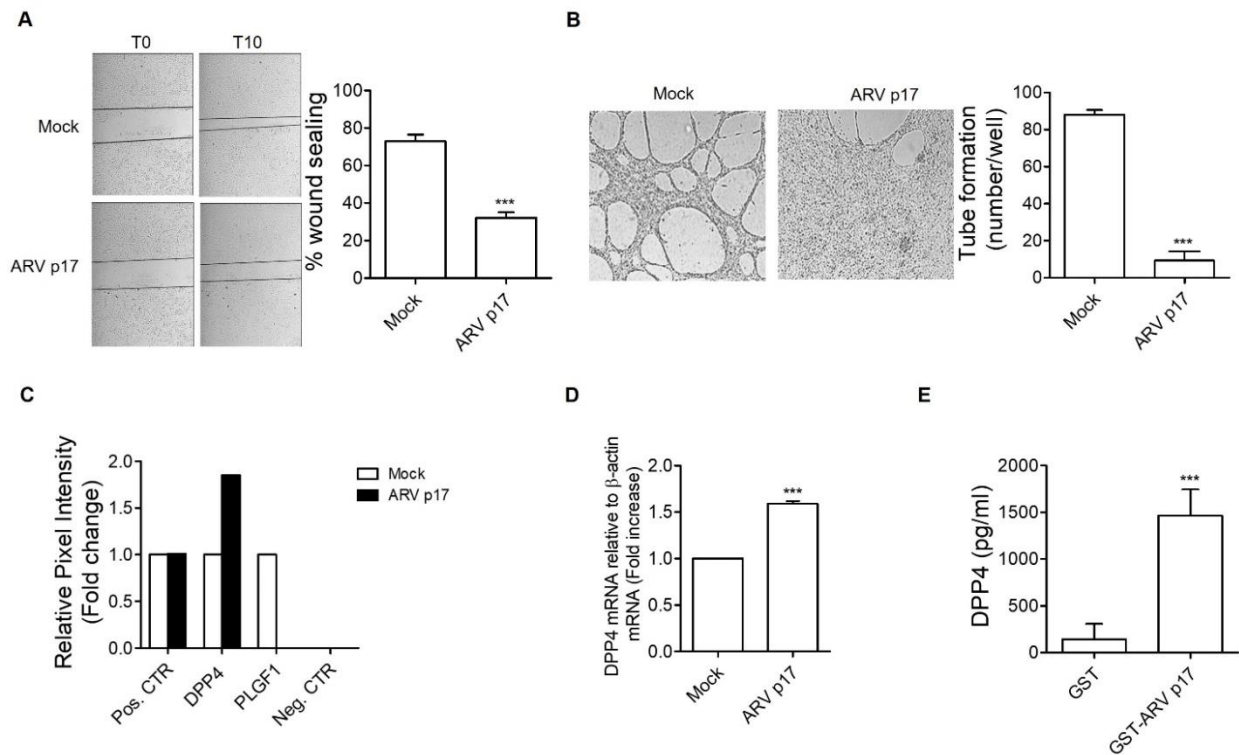
Fig. 13 **ARV p17-mediated release of DPP4 expression** (**A**) Wound healing assay performed after HUVECs overnight stimulation with conditioned medium from Mock- or ARV p17-nucleofectedHUVEC cells. Confluent cell monolayers were scratched using a 200 μl pipette tip and cell migration was recorded by light microscopy 10 h after wound scratch (original magnification,4x). The wound width was measured and the relative wound area was calculated as the ratio of the remaining area at 10 h time point to 0 h starting point. Pictures are representative of one out of two independent experiments with similar results. Values are the mean ± SD of one representative experiment out of two independent experiments, performed in triplicates. (**B**) Tube formation assay performed with HUVECs co-cultivated for 48 h with Mock- or ARV p17-nucleofectedHUVEC cells. The pictures were taken 6 h after cell seeding (original magnification, 4×). Closed rings were counted as a parameter for quantification of tube formation. Pictures are representative of one out of two independent experiments with similar results. Values are the mean ± SD of one representative experiment out of two independent experiments, performed in triplicates. (**C**) Angiogenesis array performed with the supernatants of Mock- or ARV p17-nucleofected cells recovered 24 h post nucleofection. Relative pixel intensity was calculated using ImageJ software and expressed as the mean of duplicate dots. (**D**) Analysis of DPP4 gene expression performed using quantitative real-time PCR in Mock- and ARV p17-nucleofected cells. Analysis of real-time PCR data was performed with the 2^{-DDCt} method using relative quantitation study software. Quantification of DPP4 mRNA was normalized according to the internal β-actin control. Bars represent the mean ± SD of one representative experiment out of two independent experiments, performed in triplicates. (**E**) sDPP4 levels in supernatants of HUVECs stimulated with GST-ARV p17 for 48 h was quantified with human CD26 ELISA. Supernatant from GST stimulated cells was used as a negative control. Bar graph displays the absorbance observed for DPP4 concentration. Values are the mean ± SD of one representative experiment out of three independent experiments, performed in triplicates. Statistical analysis was performed by Student's t test. *** P < 0.001.

4.11 DPP4 mediates ARV p17 activities on HUVECs

We investigated whether ARV p17 inhibitory effects were mediated by DPP4 by selectively blocking its release through a specific inhibitor namely, Diprotin A (DPA). To this end, HUVECs were either pretreated with conditioned media from ARV p17-expressing ECs or with recombinant GST-ARV p17. Mock and GST pretreated cells were used as negative controls, respectively. Then, wound healing assay was carried out by incubating pretreated HUVECs with an optimal concentration of DPA (10 μM).

As expected, ARV p17 lead to a pronounced impairment in wound repair ability (ARV p17 conditioned media: $51 \pm 1\%$ and GST-ARV p17 pretreatment: $42 \pm 1\%$); whereas the addition of DPA to the former neutralized this effect significantly (ARV p17 conditioned media+DPA: $80 \pm 8\%$ and GST-ARV p17 pretreatment + DPA: $66 \pm 1\%$) (Figure 14A-B), thus suggesting an involvement of DPP4 in ARV p17 anti-migratory activity.

To further assess the involvement of DPP4 in ARV p17-mediated activities, tube formation assay was performed in the presence of DPA after GST-ARV p17 pretreatment. As shown in Figure 14C, ARV p17-inhibition of capillary-like structure formation was significantly reversed in the presence of the specific inhibitor of DPP4. The presence of DPA in medium of GST-ARV p17 pretreated ECs accounted for around 41% increase (60 ± 1) of ECs tube formation as compared to GST-ARV p17 pretreated ECs alone (35 ± 2). No significant effect was observed when ECs were pretreated with GST. Superimposable results were obtained in spheroids generated by GST ARV p17-pretreated HUVECs and cultured with DPA (25 ± 1) as compared to GST-ARV p17 pretreated ECs alone (11 ± 1) (Figure 14D). These findings suggest that ARV p17 anti-angiogenic and anti-migratory activities are strongly supported by the release of DPP4.
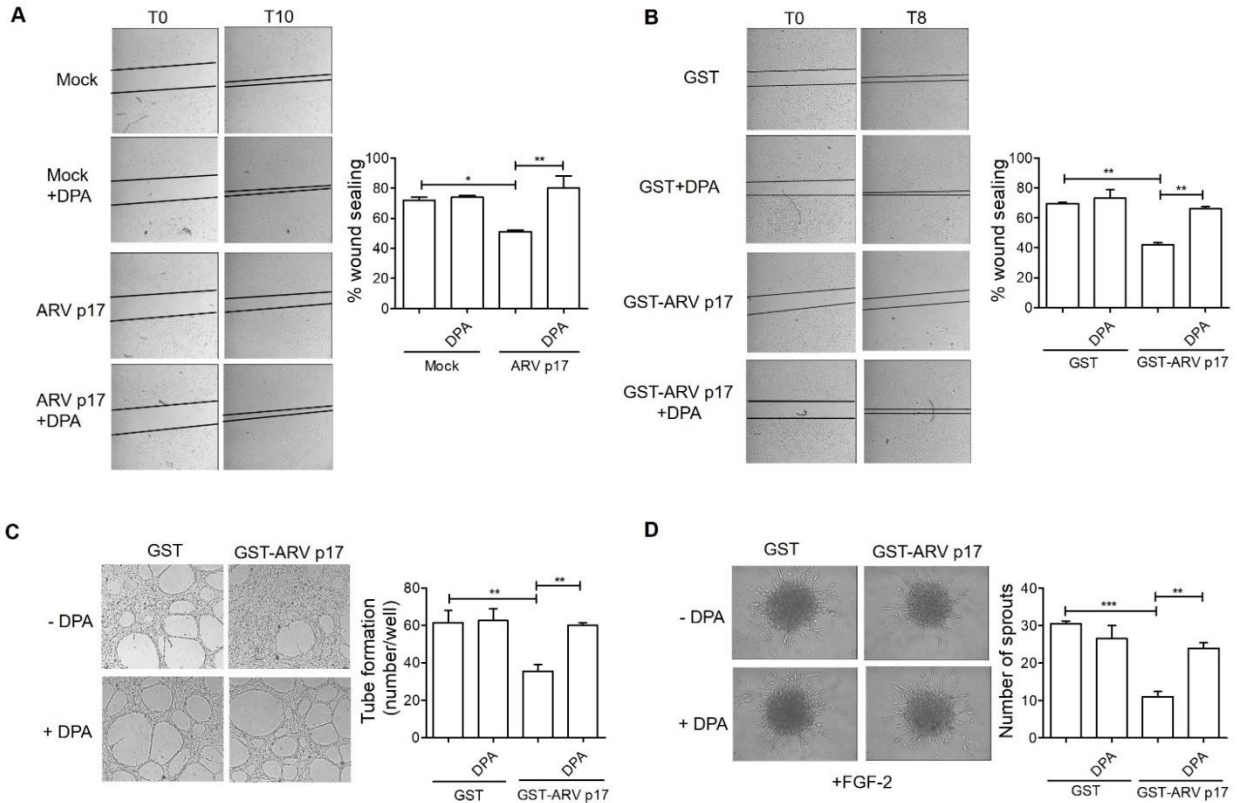
Fig. 14 **Effect of DPA on ARV p17 activities** (**A**) Wound healing assay in the presence of DPA (10 μM) to assess migratory activity of ECs pretreated with conditioned medium from Mock- and ARV p17-expressing cells (original magnification, 4x). The wound width was measured and the relative wound area was calculated as the ratio of the remaining area at 10 h time point to 0 h starting point. (**B**) Wound healing assay in the presence of DPA (10 μM) to assess migratory activity of ECs pretreated with recombinant GST or GST-ARV p17 (10 ng/ml) (original magnification, 4×). The wound width was measured and the relative wound area was calculated as the ratio of the remaining area at 8 h time point to 0 h starting point. (**C**) Tube formation assay in the presence of DPA (10 μM) to assess capillary-like structures formation in GST- and GST-ARV p17 pretreated cells. Pictures were taken after 6 h of culture (original magnification, 4×). Closed rings were counted as a parameter for quantification of tube formation. (**D**) 3D spheroid assay in the presence of DPA (10 μM) and FGF-2 (100 ng/ml) to assess sprout formation in GST- and GST-ARV p17 pretreated cells (original magnification, 20×). The bar graph shows the average number/spheroid of EC sprouts. Pictures are representative of one out of three independent experiments with similar results. Values are the mean ± SD of one representative experiment out of three independent experiments, performed in triplicates. Statistical analysis was performed by one-way ANOVA and Bonferroni's post-test was used to compare data. * $P < 0.005$; ** $P < 0.01$; *** $P < 0.001$.

4.12 ARV p17 inhibits angiogenesis through DPP4 release in lung ECs

Since ARV p17 has been proven to exert anti-carcinogenic activity on human lung cancer cells amongst others [20], we wondered if the viral protein could be active in human microvascular endothelial cells of lung origin. To this aim, we performed key experiments by using HMVECs either nucleofected or pretreated with GST-ARV p17. As shown if Figure 15A, ARV p17-expressing HMVECs lost their ability to form capillary-like structures when seeded on a Matrigel coated well (35 ± 1), compared to Mock (63 ± 3), demonstrating the ability of the viral protein to inhibit angiogenesis in microvascular endothelial cells. Interestingly, ARV p17-expressing cells were also able to counteract the activity of the pro-angiogenic FGF-2 (18 ± 1), as demonstrated by HMVECs spheroid assay (8 ± 1) (Figure 15B). At the same time, as shown in Figure 15C, GST-ARV p17 was able to inhibit the activity of the potent pro-angiogenic factor VEGF-A (15± 3 sprouts) as compared to GST (37± 1sprouts).

In order to understand if the mechanism behind the ARV p17 activities on HMVECs were the same as of HUVECs, we straight attempted to inhibit the former through DPA. Incubation of GST-ARV p17 pretreated cells with DPA strongly inhibited its anti-angiogenic properties as demonstrated by capillary-like structure formation assay (46 ± 2) (Figure 15D) and spheroid assay (16 ± 1) as compared to GST-ARV p17 with relatively lower number of tubes (19 ± 1) and sprouts (7± 1) formation, respectively (Figure 15E).
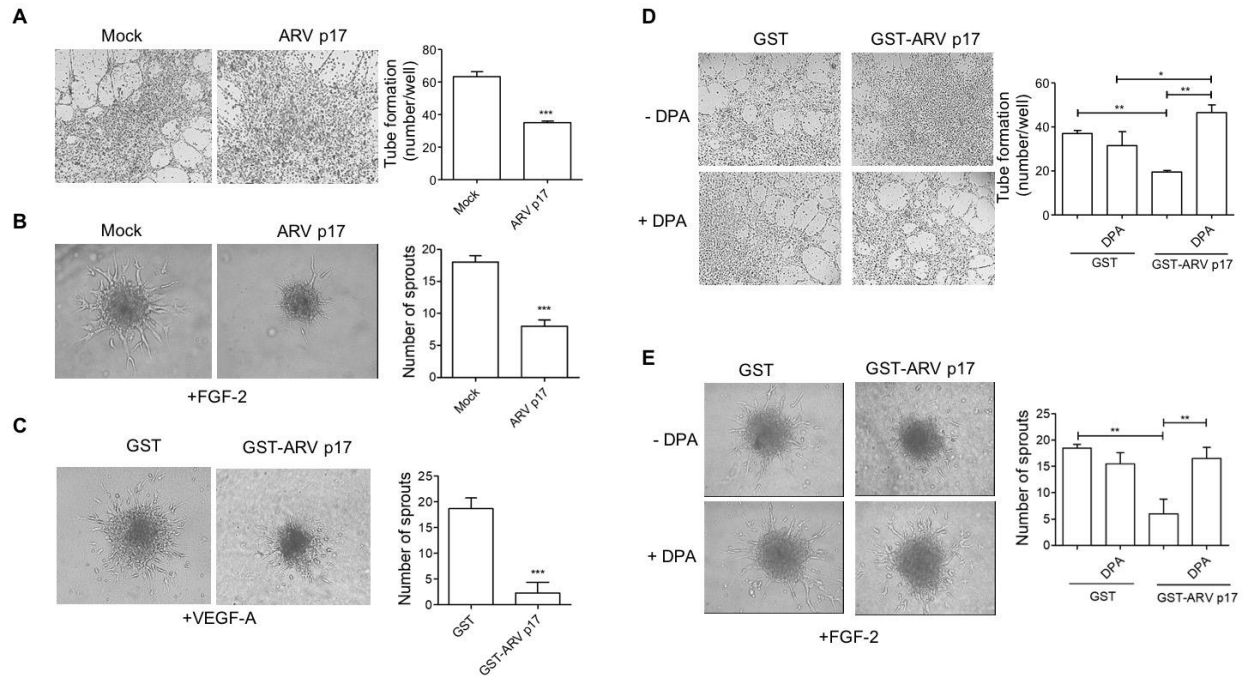
Fig. 15 **Effect of ARV p17 expression on HMVECs angiogenesis** HMVEC cells were mock-nucleofected (Mock) or nucleofected with ARV p17-expressing plasmid (ARV p17). Angiogenesis was analyzed 48 h post-nucleofection. (**A**) HMVECs were seeded on BME-coated plates. Images were taken after 6 h of HUVEC culture on BME (original magnification, 4x). Closed rings were counted as a parameter for quantification of tube formation. (**B**) Sprouting of spheroids generated by Mock or ARV p17HMVECs upon FGF-2 treatment. Pictures were taken after 24 h of culture (original magnification, 20×). The bar graph shows the average number/spheroid of EC sprouts. (**C**) HMVECs were pretreated with10 ng/ml of either recombinant GST or GST-ARV p17 for 24 h. Spheroid assay in the presence of VEGF-A (30 ng/ml) to assess sprout formation after 24 h in GST- and GST-ARV p17 pretreated cells (original magnification, 10×). The bar graph shows the average number/spheroid of EC sprouts. (**D**) Tube formation assay in the presence of DPA (10 μM) to assess capillary-like structures in GST- and GST-ARV p17 pretreated cells. Pictures were taken after 8h of culture (original magnification, 4×). Closed rings were counted as a parameter for quantification of tube formation. (**E**) 3D spheroid assay in the presence of DPA (10 μM) and FGF-2 (100 ng/ml) to assess sprout formation after 24 h in GST- and GST-ARV p17 pretreated cells (original magnification, 20×). The bar graph shows the average number/spheroid of EC sprouts. Pictures are representative of one out of two independent experiments with similar results. Values are the mean ± SD of one representative experiment out of two independent experiments, performed in triplicates. Statistical analysis was performed by Student's t test. * P < 0.005; ** P < 0.01; *** P < 0.001.

MMP's have already been shown to be involved in the shedding of DPP4 in its soluble form from the membrane of the cell surface. To identify if these proteases are also involved in the secretion of soluble DPP4 upon ARV p17 administration in endothelial cells, we used an MMP inhibitor Batimastat (20 ng/ml) to add to the cells seeded for performing a Matrigel assay. Addition of the former, to some extent, suppressed the activity of ARV p17 and, hence, metalloproteases could be involved in the secretion of DPP4 due to the presence of ARV p17 (Fig. S1A). Batimastat is a broad-spectrum inhibitor known to inhibit several proteases such as MMP-1, 2, 9, 7 and 3 amongst others. Batimastat suppressed the activity of ARV p17 in Matrigel assay, probably, contributing to the DPP4 role in the anti-angiogenic activity mediated by ARV p17, which was unable to be secreted from the membrane surface and perform its function to suppress the cell migration and tube formation.

On the other hand, when HIV p17 was added to the cells plated for Matrigel assay in a similar setting, to evaluate if p17 from ARV can suppress the angiogenic activity of p17 from HIV. To our surprise, pre stimulation with GST-ARV p17, but not GST, was able to inhibit the tube formation ability of HIV p17 adding to the broad-spectrum anti-angiogenic activity of the former viral protein. HIV p17 was always used under starved conditions (EBM+0.5% FBS, overnight) in endothelial cells (Fig. S1B). In results section, the viral protein is further elaborated on its evaluation with different pro-angiogenic factors for attesting its role as a potent anti-angiogenic molecule, in both macro and microvascular endothelial cells.

Fig. S1 (A) HUVECs were stimulated with recombinant GST- or GST-ARV p17 for 24h and seeded on BME-coated plates with Batimastat 20ng/ml. Images were taken after 12 h of HUVEC culture on BME (original magnification, 4x). Closed rings were counted as a parameter for quantification of tube formation. Images are representative of one out of three independent experiments with similar results. (B) HUVECs were s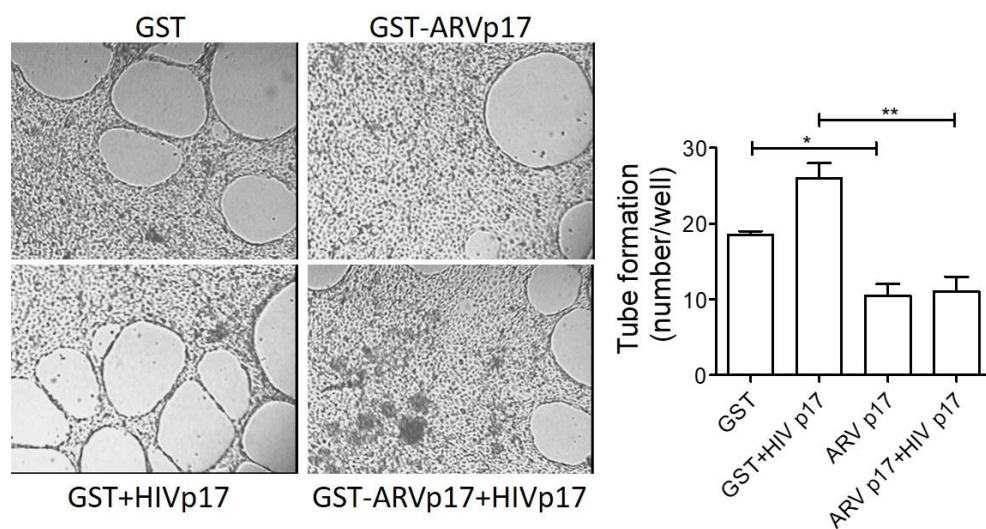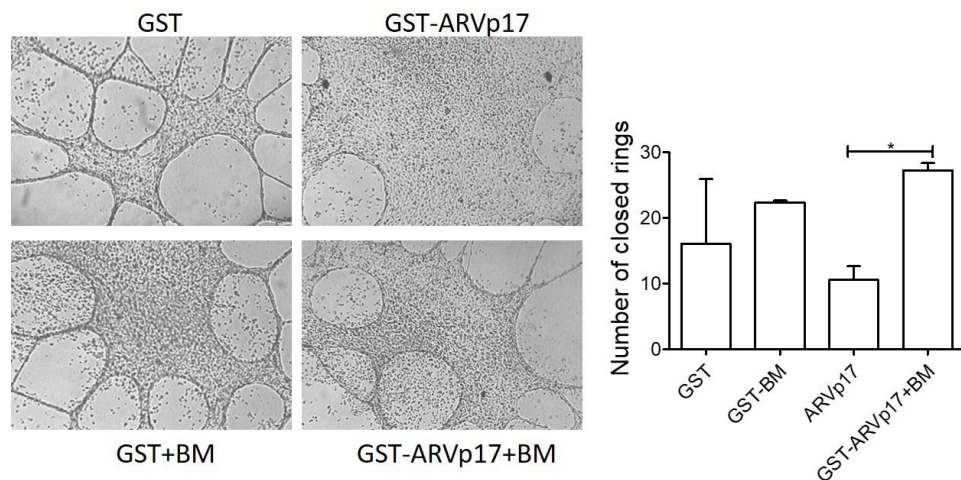timulated with recombinant GST- or GST-ARV p17 for 24h and seeded on BME-coated plates with Batimastat 20ng/ml. Images were taken after 12 h of HUVEC culture on BME (original magnification, 4x). Closed rings were counted as a parameter for quantification of tube formation. Images are representative of one out of three independent experiments with similar results.

5. DISCUSSION AND CONCLUSIONS

Avian Reoviruses (ARVs) are important pathogens, belonging to the Orthoreovirus genus in the Reoviridae family, associated with different diseases, like viral arthritis, enteric disease problems, immunosuppression and chronic respiratory disorders in many avian species [12]. The ARV genome consists of 10 double-stranded RNA-genome segments, which encode at least 10 structural proteins and four nonstructural proteins, but very little is known about the functions of the most proteins. The non-structural p17 protein of ARVs (ARV p17) is a 146 aa protein encoded by the S1 gene segment, whose ORF is highly conserved in all avian Reovirus S1 segments, and has been suggested to play an important role in virus-host interaction [13]. The ARV p17 does not show sequence similarity with any other known protein, so its sequence offers no clues about its function [16]. It is known to be a nucleocytoplasmic shuttling protein, which has been suggested to participate in cell nuclear processes, such as gene transcription, DNA binding and cell growth regulation [17,18]. The viral protein possesses the capability to translocate into the nucleus, induce autophagy and increase viral replication [39,40]. Recently, different studies have reported the capability of ARV p17 to promote a significant cell growth inhibition and cell cycle retardation in several cancer cell lines through activation of the p53 pathway and interaction with cyclin-dependent kinases (CDKs) and cyclins [20]. In particular, the direct interaction of ARV p17 with CDK1 leads to its inactivation, but also to the suppression of the Serine/Threonine-protein kinase Plk1, an early trigger for G2/M transition with oncogenic properties [21,71].

Tumor growth, progression and metastasis are driven by angiogenesis [28] and inhibition of angiogenesis has become one of the most exciting approaches in the development of anticancer therapy. Several viral structural and non-structural proteins are able to induce cell cycle arrest, display anticancer activity *in vitro* and *in vivo* [27,8,72-74] and concomitantly, potent antiangiogenic functions [7]. In this study, we investigate the properties of ARV p17 in regulating angiogenesis and demonstrate that the viral protein is able to significantly inhibit macrovascular and microvascular EC migration, capillary-like structure and sprouting angiogenesis in a 3-dimensional (3D) EC organotypic culture. Moreover, we highlight that the anti-angiogenic activity of the viral protein is exerted through the increased secretion of dipeptidyl peptidase (DPP4).

In the present study, we show the anti-angiogenic property of the non-structural viral protein ARV p17, which occurs through the increased secretion of sDPP4. In particular, ARV p17, either

endogenously expressed or exogenously administrated, is able to significantly inhibit EC migration, tube formation and sprouting *in vitro*, but also *ex vivo* and *in vivo,* as confirmed by aortic ring and CAM assays, respectively. Moreover, the viral protein is capable to suppress not only the physiological angiogenesis, but also the one induced by two different potent angiogenic promoting agents, namely FGF-2 and VEGF-A, thus indicating that ARV p17 can act as an effective wide-spectrum anti-angiogenic molecule.

Current anti-angiogenic therapies use drugs which specifically target only a single proangiogenic molecule, even though tumors can activate alternative pathways to stimulate angiogenesis [75].In particular, the most important and best-characterized pro-angiogenic molecular factors and signaling pathways involved in tumor neoangiogenesis are the members of the VEGF-family, which are expressed at high levels in most tumors and involved in conditioning the microenvironment to impact on EC angiogenic activity [76]. Therefore, VEGF-mediated signaling has become one of the most promising anti-angiogenic therapeutic targets in oncology for clinical treatment of human cancers and metastasis [77], even when it's not difficult to find acquired or intrinsic therapy resistance associated with anti-VEGF monotherapeutic approaches. To date, a crucial need remains for the introduction of a next generation of anti-angiogenic drugs which could block simultaneously different pro-angiogenic pathways by showing a wide clinical efficacy [78]. Within this context ARV p17, by simultaneously interfering with both VEGF and FGF-signaling cascades, could represent a new drug to be used alone or in combinations with other drugs, in producing an effective anti-cancer activity. It is worth noting that the mitogenic activity of FGF-2 is significantly more powerful than that of VEGF-A [79]. Since FGF-2 is involved in the resistance to VEGF-inhibition [80–82], it represents a novel target for anti-angiogenic drugs possibly endowed also, as for ARV p17, with a simultaneous anti-VEGF activity.

Numerous proteins and chemical molecules have been found to inhibit angiogenesis, but the underlying mechanism of their action is poorly understood and their outcome in clinical trials remains unpredictable or sometimes, disappointing [83]. In this study, we highlighted the molecular mechanism by which the viral protein ARV p17 exerts its anti-angiogenic activity. In particular, we identifiedDPP4/CD26, a serine exopeptidase expressed on different HMVECs(i.e. in liver, spleen, lungs and brain) [84], as the molecule responsible for the ARV p17 antiangiogenic function. DPP4 is mainly anchored onto the cell membrane and then released in an active soluble

form(sDPP4) in the culture supernatant and in different biological fluids [85–87.] In our study, we demonstrate that ARV p17 increases sDPP4 in the ECs supernatants by a still uncovered mechanism. Matrix metalloproteases and kallikrein-related peptidase 5 have been implicated in its shedding [67,88]. Studies are warranted in the future to understand the role of these molecules in the ARV p17-induced sDPP4 release.

DPP4 is a multifunctional protein, which possesses the capability, through its intrinsic peptidase activity, to inactivate or degrade many substrates, including chemokines involved in cell migration and tumor metastases [89,90]. Currently, it is not easy to exactly determine its role in carcinogenesis, since it can act as a tumor promoter or suppressor [84,91]. Its role depends essentially on tumor type and localization, cell type and microenvironment. However, DPP4 displays an anti-oncogenic function in those tumors linked to the CXCL12/CXCR4 axis, which is known to support neovascularization, tumor growth and metastasis during cancer development [92–96]. In this context, different studies suggested that CXCL12 degradation by DPP4 is involved in the metastatic process [97,98] and that the removal of two N-terminal amino acids from CXCL12 reduces the chemokine affinity for CXCR4 receptor and, consequently, its activity [99,100]. Moreover, DPP4 is known to suppress angiogenesis by directly interacting with CXCR4 and downregulating its mRNA and protein level [87]. Different studies highlighted that inhibition of tumor progression also occurred in the absence of DPP4 enzymatic activity [87,101] or an increased DPP4 gene expression being sufficient to revert the malignant tumor phenotype [86,87,102,103]. Therefore, we can hypothesize that the increased DPP4 mRNA expression triggered by ARV p17 (Figure 8D and 9D) may also play a role in modulating the CXCL12/CXCR4 axis to impair angiogenesis. Moreover, our results showing the capability of ARV p17 to block FGF-2-induced angiogenesis through the involvement of DPP4 are in line with the previous studies showing the ability of DPP4 to inhibit the malignant phenotype of prostate cancer cells by blocking FGF-2 signaling [104].

Our data highlights also the capability of ARV p17 to totally suppress the release of the pro-angiogenic molecule placental growth factor (PLGF1) (Figure 8C). At present, it is unknown if a role exists for DPP4in controlling PLGF1 expression. At the same time, we cannot exclude that the lack of expression of PLGF1 may be, at least in part, responsible for the ARV p17 anti-angiogenic effects [105,106]. Both hypotheses need to be explored in future studies.

At the best of our knowledge, the ability of ARV p17 to condition the microenvironment and impact on angiogenesis through an increased expression of sDPP4 is completely new and suggests a peculiar activity of the viral protein. ARV p17 is known to inhibit cell growth of different cancer cell lines both *in vitro* and *in vivo* by triggering cell cycle retardation [105]. Thus, the "two compartments" activity of ARV p17 may provide anticancer therapeutic benefits not only in terms of oncosuppressive effects on tumor cells but also by inhibiting the neovascularization process, hence hampering the tumor parenchymal/stromal cross-talk.

In conclusion, the complex antitumor activity of ARV p17 may open the way to a new promising field of research aimed to develop new therapeutic approaches for treating tumor and cancer metastasis.

In this study, given the involvement of ARV p17 in cell growth and tumorigenesis, we explored its capability to regulate angiogenesis and vasculogenesis, which are fundamental processes in tumor growth. Our data highlights that ARV p17, either endogenously expressed or exogenously administrated, can act as an effective anti-angiogenic moleculeon ECs byalso suppressing the angiogenesis mediated by two potent inducers, such as VEGF-A and FGF-2. Moreover, we demonstrate that ARV p17 exerts its anti-angiogenic function through DPP4 action.

Overall, our findings define this viral protein as a promising drug to develop new therapeutic approaches for cancer therapy.

6. Emerging Viral Proteins And Future Perspectives

For several ages, viruses have largely been known for induction and progression of cancer by modulating the activity of cellular proteins or by expressing their own pro-carcinogenic factors. e. g. viruses like EBV and KSHV mediate the release of factors like COX-2, TP (thymidine phosphorylase), and angiogenin which are involved in the release of pro-inflammatory chemical messengers and perturbates the balance between pro-angiogenic and anti-angiogenic cellular state. In the last few decades, several other viruses with anti-carcinogenic functions have emerged with the possible abilities to arrest the cell cycle, mediating apoptosis, or even releasing anti-angiogenic factors to regulate the hyperinflammatory cancerous state, by shifting the balance towards an anti-inflammatory environment. Finding such viruses and importantly, viral components that mediate cancer suppression effects, without any collateral adverse effects on normal cells, could prove to be a booster in cancer therapy. The ability of virus infection to lyse the cells and to stimulate an effective immune response against the antigens present on tumor cells for generating long-lasting immunity has been employed for a long time to use in oncolytic virotherapy. Anti-cancer agents specifically target cancer cells by exploiting the same cellular defects that promote tumor growth, with restricted or no productive infection to normal tissues. HSV-based talimogene laherparepvec has been proved to be the first oncolytic viral vector approved for the treatment of malignant metastatic melanoma. The anti-viral drug and viral vector therapies, although can turn over at higher levels but are limited by safety and tumor-targeting concerns.

Viruses that normally live in and among us make the genetic blueprints that enable them to act like drugs and may serve as the basis for cancer therapy. Viral genomes consist of two transcriptional units i.e., non-structural (NS) and viral particle (VP) transcription units which encode for non-structural and structural proteins, respectively. Structural proteins are components of icosahedral capsids and virus particles, such as proteins of cylindrical viruses or different components of tailed phages; and viral enzymes such as viral proteinases, and RNA and DNA polymerases; important for functions like cell recognition, fusion, entry, replication, whereas non-structural proteins have been involved with cellular hijacking mechanism like inclusions formation, cytoskeleton interaction, apoptosis, and autophagy, but not all NS proteins are known for their functions. Since p53 is found to be mutated in several cellular cancers, proteins exerting multiple cell death pathways, other than p53 activation, may prove to provide

better and efficient treatment in a holistic way. Several non-structural Rep proteins, known for their involvement in virus replication cycle and latency, have been characterized from different parvoviruses for their benevolent roles like adeno-associated virus AAV Rep78 has been shown to possess anticancer properties via cell cycle regulation, and has homologous counterparts in other viruses like human herpes virus HHV-6A Rep6 (U94), HCMV (human cytomegalovirus) r127, and avian parvovirus Rep1/2 which shares the most homology with Rep68/78. These proteins are also expected to share functional homology with each other but so far, only HHV-6 Rep6 has been reported to be sharing striking functional similarities with Rep78.

We are not yet completely familiar with the functions of all of the viral proteins participating in cancer suppression and their respective regulatory mechanisms in a cancer microenvironment, but below enlisted molecules are potential subjects to explore and may pave the way to be functional candidates in oncotherapy. Collectively, viral structural and non-structural proteins are known to play a role in modulating different cellular mechanisms and targeting the tumor cells, which sounds like a promising alternative to the use of the whole virus or viral vectors to exert anti-oncolytic activities and may prove to be efficient and safer virotherapy.

 Avian viruses

Avian viruses are known to cause morbidity and mortality including diseases like viral arthritis, hepatitis, respiratory syndromes, pericarditis, immune suppression, enteric diseases, and even sudden death in species like goose, ducks, turkey, pigeons, pheasants, raptors, and quails, but not in humans. The economy and poultry industry has been affected in several countries due to these viruses. Animal-derived viruses that do not circulate extensively in the human population represent a potential source of viral proteins that enable bypassing pre-existing immunity. Due to which they might prove to be safer and effective candidates to be utilized in cancer therapy with lesser side effects as compared to conventional viral vectors with efficacy and processing risks. Interestingly, the nuclear localization property of avian viral proteins makes them effective in targeting cellular mechanisms. In the next section, we have summarized some of the newly emerged avian viral proteins which are recently emerged for their potential functions and may prove to be effective anti-carcinogenic agents in the future.

- CAV Apoptin

Chicken anemia virus (CAV), a member of the genus Gyrovirus, is an etiological agent of chicken infectious anemia known to cause immunosuppression in young chickens and compromised immune response in older birds by infecting hematopoietic cells including bone marrow-derived cells [107, 108], myeloid progenitor cells and T-lymphocyte precursor cells[109]. VP3, a structural14 kDa, 121-amino acid protein from CAV is known for its property to induce apoptosis and viral cytotoxicity in host cells, hence the name, Apoptin[110]. The C-terminal domain of apoptin contains a bipartite nuclear localization sequence (NLS 82-88; 111-121) and a secondary nuclear export sequence (NES; 97-105), and together, these motifs confer the nucleocytoplasmic shuttling activity of the protein[111,112]. Apoptin is known for its multimerization and nucleus retention activity in tumor cells due to its interaction with cellular proteins like APC/C and transporting the latter from cytoplasm to nucleus, to be deposited in PML-nuclear bodies, owing to its shuttling activity but remains cytoplasmic in normal cells. Apoptin is commonly phosphorylated at Thr-108, with a role to play in the toxicity, however not necessary for nuclear localization of apoptin in tumor cells [111, 113, 114]. Though, mutations in LRS lead to reduced nuclear accumulation. In normal cells, apoptin has been shown to be localized in the cytoplasm, aggregated, and eventually degraded [108]. Therefore, Apoptin has the ability to selectively kill various human tumor or transformed cells with little cytotoxic effect in normal cells.

Mechanism of Action

Apoptin triggers caspase-dependent cell death via the intrinsic apoptotic pathway [115,116], independently of p53 but requires pro-apoptotic TAp73 isoforms from p53 family [117, 118]. Like NS1, DDR (DNA damage response) signaling plays a key role in nuclear localization and apoptosis induction [119]. Inhibition of Chk1 and Chk2 kinases in chicken lymphoblastoid cells resulted in cytoplasmic re-localization of apoptin, thereby suggesting phosphorylation of the residues T56 and T61 are important for regulating the localization and apoptotic activity without affecting other activities of the protein [120]. Studies have found apoptin to trigger the nuclear accumulation of the related kinase Akt in prostate cancer cells [121] and PKCβ1 in colon cancer cells, likely via N-terminus located region [122] suggesting PKCβ1 to be a tumor-specific target responsible for sensitizing cells to Apoptin in colon cancer cells, while normal colon mucosa

cells remained resistant [123–125]. Apoptin also drives translocation of Nur77, another transcription factor, into the cytoplasm from the nucleus where it causes MOMP (mitochondrial outer membrane permeabilization) and induces cytochrome c release mediating intrinsic cell death pathway [117.] Other studies have shown that apoptin interacts and inhibits Abl/BCR-Abl1 and its various downstream targets like STAT5, CrkL, and c-myc [126].

Jangamreddy et al. designed an apoptin-derived decapeptide (amino acids 81-90, spanning apoptin interaction domain) as an alternative therapeutic agent, described in the next subsection, which leads to inhibit BCR-Abl1 downstream target c-myc with comparable efficacy to full-length apoptin for the treatment of CML leukemia, efficiently than drug-associated chemotherapy. They demonstrated the activation of cell-penetrating conjugate Tat-apoptin in BCR-Abl1 expressing murine human cell lines binds to the SH3 domain of BCR-Abl1, without affecting normal cells, and inhibits its activity by possible prevention of SH1 kinase domain activation [127].

AdP

Apoptin derived peptide (AdP) as described by Zhang et al. in 2017, is a 5.2 kDa peptide with an isoelectric point of 13.18, hydrophilic, highly soluble, consists of four parts: a penetrating peptide Tat (for entering facilitation), the core NLS1, LRS (the flexible connection between NLS1 and NLS2) and NLS2 sequences [128]. The peptide was designed so, for its nuclear accumulation and direct targeting to cancer cells. Owing to its smaller size, the peptide was designed to exhibit reduced immunogenicity and strong antitumor activity against glioma cells. The molecule led to reduced HSP70 mRNA and protein levels in tumor cells and proved to be more effective in mediating glioma cell apoptosis than the apoptin itself *in vitro* and *in vivo* by interacting with the HSE domain. However, compared with apoptin, apoptin-derived peptide increased apoptosis in human astrocytes, but to a lower extent than glioma cells [128]. Furthermore, the combination of drug treatment with AdP may reduce drug resistance and could be an effective method for GBM treatment. Interestingly, down the line, Hou et al. demonstrated that recombinant apoptin protein (GST tagged Apoptin, chemically modified by folic acid for entering into the cells) inhibits the growth of breast cancer cells likely by apoptin mediated apoptosis. They demonstrated that rApoptin inhibits proliferation and induces apoptosis *in vitro* following similar molecular mechanisms as Apoptin by crossing the membrane of cells and

leading to cell apoptosis by facilitating the expression levels of Bax, Cyt c, p-Akt, and p-Nur77 [129]. On the other hand, Yuan et al. previously showed that apoptin induces mitochondria-mediated caspase-3 dependent cell death in cancer cells [130, 131]. Later, they reported that apoptin and AdP specifically interact with the SH3 domain on HSE in the promoter of HSP70. They postulated the potential mechanisms for AdP mediated inhibition to be linked with inactivation of the RTK/PI3K/Akt pathway and suppression of MMP-9 expression [132]. Another study showed that AdP inhibited cell viability in chemotherapy drug-resistant gastric cancer cells, without effecting normal cells by PI3K/Akt/ARNT signaling pathway. Nevertheless, the studies related to the apoptin derived peptide needs to be further elucidated. The same group suggested that AdP can increase the G2/M phase population, thereby leading to apoptosis, and AdP-treated chemotherapy-resistant cells displayed an increased sensitivity to the therapy as compared to apoptin, possibly by reducing the levels of p-AKT, p-p85, AKT, and p85 in both therapy sensitive as well as resistant cells [133]. Collectively, these findings suggest that the peptide could be used in combination with other drugs and targeted for different kinds of cancer therapy, provided the safety of normal cells has been assured.

- MDRV p10.8

Muscovy duck reovirus (MDRV) is another member of the genus Orthoreovirus, an important poultry pathogen that is involved in several diseases including viral arthritis, growth retardation, pericarditis, enteritis, hepatitis, respiratory syndromes, and sudden death. Ducklings infected with the reovirus were first reported in 1950 and Muscovy duck reovirus (MDRV) was first isolated in 1972 [134]. Its genome consists of 10 double-stranded RNA segments which can be separated into three size classes: L (large), M (medium), and S (small). Like avian reoviruses, MDRV appears to evolve mechanisms that alter the physiology of host cells during infection to increase its own replication. MDRV was first appeared to induce autophagy in chicken fibroblast cells via suppression of mTOR phosphorylation by σNS nonstructural protein-induced autophagy by exhibiting marked increased levels of LC3-II [135]. MDRV p10.8 is coded by the S4 gene sequence and is found highly conserved suggesting that p10.8 plays an important role in virus-host interactions. This polypeptide has no significant sequence similarity to other known proteins, so its amino acid sequence offers no clues about its function [136].

Similar to p17 from avian reovirus and σ1s from mammalian reovirus (MRV), p10.8 is able to localize to the nucleus independent of the host cell type or viral infection, based on a signal mediated import, though their NLS's has no sequence similarity. It has an aromatic amino acid-rich NLS which enables it to pass through the Nuclear pore complex (NPC) and a leucine-rich NES [137]. Recently, MDRV p10.8 has garnered attention due to its apoptosis-inducing ability in an avian immortalized fibroblast cell line (DF-1) and Vero cells unlike syncytium formation activity of the homologous proteins in ARV, NBV (Nelson Bayvirus), and MRV (Mammalian Reovirus).

Cell cycle arrest

ARV σC-induced apoptosis was shown to be associated with p53 and mitochondrial pathway [138] and Bip/GRP79-mediated Bim, an apoptosis regulator, translocation to the ER [139]. At the same time, p10.8 induced apoptosis is associated with ER stress through the BIP/IRE1/XBP1 pathway. The viral protein (p10.8) dissociates the Bip/IRE1 complex and increases the phosphorylated form of IRE1 to activate XBP1 as indicated by the increased mRNA levels of Bip, XBP1, CHOP, and caspase-3 in MDRV-infected cells. Another study revealed that p10.8 induced cell cycle arrest at the G0/G1 phase in DF-1 cells as p10.8 caused BiP to dissociate from PERK and increased the phosphorylation levels of PERK (protein kinase R-like ER kinase) and eIF2α, which led to the progression of ER stress and eventually, cell cycle arrest.

To summarize, the viral protein increases the protein expression of BiP, p-PERK, p-eIF2α, CHOP (C/EBP-Homologous protein), cleaved-Caspase12, and cleaved-Caspase3 indicating that p10.8 protein induces cell apoptosis-related to ER stress [134, 140]. These findings imply a cell cycle-regulated role of p10.8 in inducing apoptosis and eventually cell death in mammalian and avian cell lines which could prove to be effective in oncotherapy in tumor cells, owing to its similarity with p17 in PKR activation and nuclear localization, in the absence of any cytotoxic effects to human cells. Furthermore, high levels of kinases in cancerous cells may facilitate high specificity of action for p10.8. Recently, it has been demonstrated that both MDRV p10.8 and ARV σC mediate CDK4 degradation via the ubiquitin-proteasome pathway, though neither p10.8 nor σC directly interacts with CDK2 or CDK4, by stabilizing Cdc20 with the aid of molecular chaperones CCT2 and CCT5, to mediate cell cycle arrest and p10.8-induced apoptosis [141]. On the other hand, the fact that both p10.8 of MDRV and σ1s of mammalian reovirus can localize to the nucleus and cause apoptosis of infected cells suggests that σ1s and p10.8 may be

functionally related [136]. Nuclear import of p10.8 mediates activation of p53 probably via suppression of nucleoporin Tpr in Vero cells through activation of the nucleoporin Tpr/p53 as in the case of ARV p17 followed by the activation of extrinsic cell death Fas/caspase 8/caspase 3 pathways. This property of the protein to modulate different apoptotic and cell cycle control pathways could make it a suitable candidate for targeting tumor cells. However, further characterization of the protein is required, given the limited studies reported for the same, for bringing it to therapeutic use.

- Old World (OW) Alphaviruses

Alphaviruses belong to the family Togaviridae, are single-stranded non-segmented positive-strand enveloped viruses with an icosahedral structure [142]. OW alphaviruses include Sindbis Virus (SINV), Semliki Forest Virus (SFV), and chikungunya virus (CHIKV) share many common characteristics. Nearly all the alphaviruses are arthropod-borne and are transmitted to their vertebrate hosts by mosquitoes [143]. The naturally occurring old world alphaviruses are relatively milder in humans and severely infect species like birds, horses, or cattle. Alphaviruses are known to target lymph nodes. A single viable virus particle of replication-competent wild-type Sindbis virus could potentially kill an entire tumor if it replicates and spreads efficiently throughout the tumor mass [144].

Cell cycle regulation by alphaviruses

Sindbis virus (SINV) is an RNA virus and is transmitted to birds and mammals by mosquito bites [145] which subsequently spreads throughout the body via the bloodstream [146]. In humans, SINV infection is considered to induce no symptoms or only mild symptoms (fever, rash, and arthralgia) suggesting low infectivity and viral replication in normal tissues. SINV was observed to induce cytopathic effects in ovarian and cervical cancer cell lines without affecting normal keratinocytes. It was found to be stable in the bloodstream and effective in targeting remote tumors as shown by regression of cervical tumor xenografts in SINV infected mice [143]. The virus-induced cell death in human squamous carcinoma, HSC-3 cells due to apoptosis, possibly related to caspases-3, 9, cytochrome c, NF-kB, IkBa, and IKK regulation [147], and neuroblastoma regression in nude mice upon intratumoral and intravenous administration of SINV AR339 strain as well as in neuroblastoma cell lines [148].

On the other hand, in Hela cells, SINV infection regulated the cell cycle progression by accumulating cells in the S phase and relatively shortening the G1 phase, by exerting up-regulation of cyclin E and Cdc25A, CDK4/6, and downregulation of p21 during the early phase of infection and facilitating quick entry into S phase, and suspension of virus proliferation in M phase. S phase was found to be arrested during the later stages of infection as SINV infection reduced the levels of cyclin A at late stage [149].

Another recently emerged naturally occurring oncolytic alphavirus, M1 is a Getah-like alphavirus (GLV) with a small genome of 11.7 kb, composed of a single positively-stranded RNA[150]. GLV predominantly provokes a mild, self-limited mosquito-borne illness in horses [151]. M1-infection in glioma cells mediated apoptosis due to G1/S-checkpoint abrogation by causing p21 deficiency leading to activation of CDK2, cyclin D1, and caspase-3 which were suppressed on activation of p21duirng later stages of infection as SINV. The virus also led to mediate mitochondrial apoptotic pathway as it causes the release of cytochrome c in the cytosol in glioma cells by caspase-3 activation likely due to an increase in the Bax/Bcl-2 ratio and free amounts of Bax. Moreover, a decrease in p21 levels was found independent of p53 levels. Bick et al. revealed that the M1-selective replication and oncolysis was ZAP deficiency dependent as ZAP, a host ISG, inhibits the replication of alphaviruses, hence the viral toxicity is cancer-selective[152]. M1inhibited viability of primary human hepatic and colorectal tumor explants administrated intravenously into immunocompetent mouse models leads to high tumor tropism and proved to be exceptionally safe and asymptomatic. Moreover, IREα1 inhibition increased M1-induced apoptosis as observed by downregulated Ki67 expression, a cell proliferation marker, while it did not affect M1 replication [153]. Later, the same group demonstrated that combined treatment of M1 with PKA inhibitor may lead to suppression of tumor growth *in vitro* through ER stress-induced apoptosis and *in vivo* through inhibition of NF-kB pathway[154]. Recently, M1 has been reported to repress orthotopic-invasive bladder cancer growth and improve the survival of tumor-bearing mice by inducing apoptosis, displaying lower levels of Ki67 and higher levels of cleaved caspase-3/7 [155] suggesting M1 to function via pleiotropic pathways to ensure its efficacy as a promising candidate.

E1/E2 structural proteins

Semliki Forest virus (SFV) is an enveloped, single-stranded, positive-sense RNA virus, another member of the genus Alphavirus; usually considered avirulent in humans but neurotropic in mice

and rats[156]. The SIN and SFV genomes encode three or more structural proteins (mainly, a capsid protein and two surface glycoproteins, E1 and E2) and four non-structural proteins (nsP1-4) that are essential components of the viral replicates and transcriptase[157, 158]. The nsP1 protein is involved in the minus strand and 26S mRNA synthesis along with nsP3 which is conserved among alphaviruses. The former also interacts with nsP4, which is an RNA-dependent RNA polymerase and affects host cell-dependent replication[159]. In many viral proteases, the efficiency of cleavage at a particular site of the polyprotein is dependent on the sequence on either side of the cleavable bond. nsP2 possesses a protease activity and is responsible for cleaving the non-structural polyprotein between nsP2 and nsP3. nsP2 is known for viral-induced cytotoxicity, shutting down cellular transcription, translation, and inducing cell death. The partial transport of nsP2 into the nucleus of SFV-infected cells has been hypothesized to trigger the mechanisms determining the cytopathogenicity of SFV infection[159]. There has not been shown any strict correlation between nuclear localization of nsP2 and cytotoxicity since the mutant replicons retained nuclear localization while being non-cytotoxic. Recently, it was observed that nsP2 and nsP3 proteins are responsible for the inhibition of cellular transcription and translation, respectively [143]. E2 is responsible for cellular-receptor binding whereas E1 is required to promote the fusion between viral particles and cell membranes[157]. Both of the viral structural proteins, in addition to nsP2, have been shown to play a role in alphavirus-induced apoptosis. Expression of Sindbis virus structural envelope proteins, E1 or E2 led to apoptosis in rat prostatic adenocarcinoma cells whereas nsP2 resulted in changes characteristic of apoptosis in BHK cells[160]. The non-structural region of the SFV genome was suggested to induce p53-dependent apoptosis and virus envelope glycoproteins were supposed to activate ER stress response activated apoptotic cell death, independently of caspase-12, whereas VRP (Virus replicon particles) lacking structural genes were not able to induce the same oncolytic effect[161]. It was further proved that viral structural proteins contribute to cell death by apoptosis as VRP particles showed a delay in caspase activation thereby concluding that structural proteins have a contributing role to initiate apoptotic activity in cancer cells[162]. Later, Hurtado et al. investigated the functional amino acids of E2 envelope protein in AR-339 Sindbis virus strain and identified that the change of amino acid E70 to K70 suppressed the ability of the protein to target metastatic tumor implants of ES-2 cells intraperitoneally injected into mice, possibly due to inhibited interaction between E2 and E1 in the vector spike confirmation[163]. In a new study by

Saito et al., the authors have demonstrated that E1 induced higher cytotoxicity in neuroblastoma (NB) cells than E2. E1 and E2 heterodimers or E1 alone were able to exhibit cytotoxicity but E2 alone did not exhibit strong cytotoxicity in NB cells. Furthermore, UV-inactivated SINV virus, in the presence of structural proteins or E1 specifically, was able to induce strong cytotoxicity in human neuroblastoma cell lines as compared to normal human fibroblasts[157], testifying it to be a potent therapeutic agent. As various viral structural proteins are known to mediate carcinogenic activities, it is no wonder that some of them could also be involved in contrary functions to perform by mediating pleiotropic pathways to induce cell death in cancer.
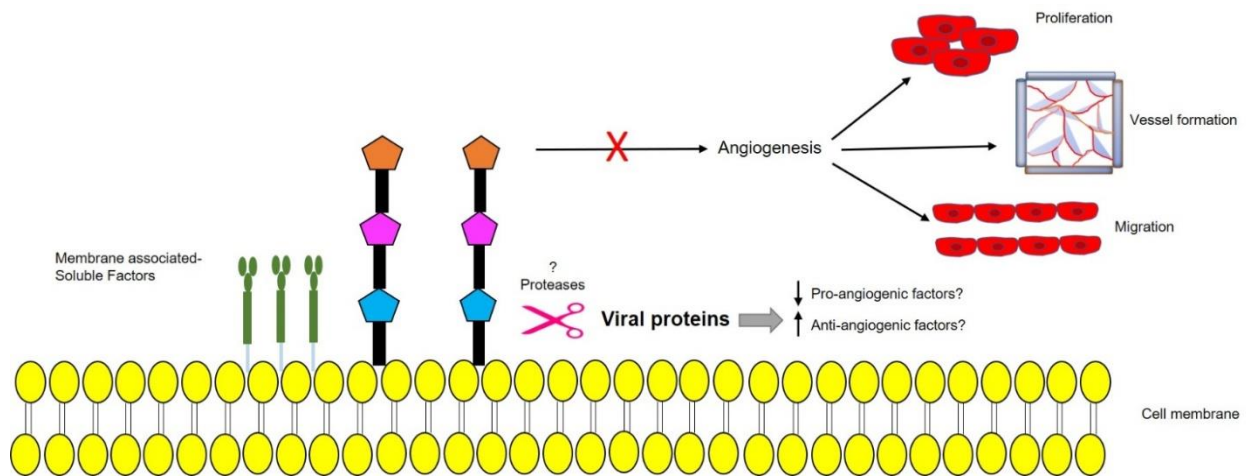
Fig. 17 Schematic representation showing possible upregulated secretion of soluble anti-angiogenic factors in the presence of viral proteins like U94 and ARV p17, leading to possible further upregulation of downstream anti-angiogenic factors, finally preventing cell migration, proliferation and vessel formation and inhibiting angiogenesis.

Protein	Host	Function	Mode of Action	Binding partners
NS1	Rat	Endonuclease, helicase, ATPase	DDR, cell cycle arrest , apoptosis	Chk2, Cdc25A, CKII, cyclin B1
Rep78	Humans	Endonuclease, helicase, ATPase	Cell cycle arrest, Apoptosis	Cyclin A, Caspase-3 cdc25A
U94	Humans	Exonuclease, helicase, ATPase	DDR, Apoptosis sHLA-G release	Caspase-9, PARP
Apoptin	Chicken	Apoptosis	Apoptosis	ChK1/2, PKC
p17	Chicken	Autophagy?	Autophagy cell cycle arrest, sDPP4 release	hnRNP A1, lamin A/C, Tpr, p53, p21, PTEN
Alphaviruses (E1/E2)	Birds, Horses Cattles	Receptor Binding Fusion	Apoptosis, ER stress response, cell cycle arrest	Caspase 3/7/9, cyclinE/ D1/C, cdc25, CDK2/4/6

Table enlisting the binding partners and their role in cancer growth suppression by viral proteins

7. Summary

Viral proteins from human and non-human sources could prove to be therapeutic molecules acting as drugs to treat cancer by stimulating extrinsic (caspase-mediated) or intrinsic (mitochondrial) apoptosis pathways and targeting cell cycle regulation. Various engineered viruses, extracted from different species including alphaviruses, are already in clinical trials for cancer therapy. Cancer cells may develop resistance to drugs and neutralizing antibodies to OVs (oncolytic vectors), but viral proteins provide a long-term cure by inducing deeper and faster molecular and cytogenetic responses, and dosage-dependent effects. The nature of anti-proliferative viral proteins does not rely on a single target but instead affects multiple cell growth pathways which make resistance development less likely. As reported in this above section, apoptosis has been a fundamental mode of action for almost all the viral proteins, independently of p53. Since, p53 has been discovered to be mutated in many malignancies and thus resistant to chemotherapy and radiation, makes this alternative therapy, even more promising. The high specificity of viral proteins for cancerous cells due to the presence of the phosphorylation residues or NLS sequences along with low pathogenicity in human cells makes them interesting candidates for cancer targeting. From mammalian viruses to avian viruses to alphaviruses, amicable viral proteins share common pathways to mediate cell growth retardation reflecting the evolution and reliability of these sources to serve as a safer and efficient therapy. Identification of such proteins and standardizing their dosage with a convenient mode of administration, by protein fusion to protein transduction domains (PTDs) or cell-penetrating peptides (CPPs), would ask for further investigation and may result in lower side effects as compared to viral vectors. Further studies could also shed light on the use of different proteins in combination as they exert similar modes of action with different pathways to contribute to a successful oncotherapy. Viral proteins like U94 and ARV p17, other than their enthusiastic participation in cancer suppression, are also responsible for regulating vessel formation by modulating the levels of secreted anti-angiogenic factors, eventually resulting in angiogenesis inhibition in multiple endothelial cell lines. As these proteins are able to circumvent any pre-existing immunity, it paves the way for successful cancer suppression, invasion, and anti-angiogenic treatment.

References

1. Vorwald, C. E., Murphy, K. C. & Leach, J. K. Restoring Vasculogenic Potential of Endothelial Cells from Diabetic Patients Through Spheroid Formation. *Cell. Mol. Bioeng.* (2018) doi:10.1007/s12195-018-0531-1.

2. Boras, E. *et al.* Monomeric C-reactive protein and Notch-3 co-operatively increase angiogenesis through PI3K signalling pathway. *Cytokine* (2014) doi:10.1016/j.cyto.2014.05.027.

3. Ludwig, N. *et al.* Tumor-derived exosomes promote angiogenesis via adenosine A2B receptor signaling. *Angiogenesis* (2020) doi:10.1007/s10456-020-09728-8.

4. Le Goff, M. M. *et al.* Opticin exerts its anti-angiogenic activity by regulating extracellular matrix adhesiveness. *J. Biol. Chem.* (2012) doi:10.1074/jbc.M111.331157.

5. Lai, C. M. *et al.* Endothelial JAM-A promotes reovirus viremia and bloodstream dissemination. *J. Infect. Dis.* **211**, 383–393 (2015).

6. Chiew, G. G. Y., Fu, A., Perng Low, K. & Luo, K. Q. Physical supports from liver cancer cells are essential for differentiation and remodeling of endothelial cells in a HepG2-HUVEC co-culture model. *Sci. Rep.* **5**, 1–16 (2015).

7. Caruso, A. *et al.* U94 of human herpesvirus 6 inhibits in vitro angiogenesis and lymphangiogenesis. *Proc. Natl. Acad. Sci. U. S. A.* **106**, 20446–20451 (2009).

8. Saudan, P. Inhibition of S-phase progression by adeno-associated virus Rep78 protein is mediated by hypophosphorylated pRb. *EMBO J.* (2000) doi:10.1093/emboj/19.16.4351.

9. Ifon, E. T. *et al.* U94 alters FN1 and ANGPTL4 gene expression and inhibits tumorigenesis of prostate cancer cell line PC3. *Cancer Cell Int.* (2005) doi:10.1186/1475-2867-5-19.

10. Van Cleef, K. W. R. *et al.* The rat cytomegalovirus homologue of parvoviral rep genes, r127, encodes a nuclear protein with single- and double-stranded DNA-binding activity that is dispensable for virus replication. *J. Gen. Virol.* (2004) doi:10.1099/vir.0.79864-0.

11. Smith, D. H., Ward, P. & Linden, R. M. Comparative Characterization of Rep Proteins from the Helper-Dependent Adeno-Associated Virus Type 2 and the Autonomous Goose Parvovirus. *J. Virol.* (1999) doi:10.1128/jvi.73.4.2930-2937.1999.

12. Lu, H. *et al.* Isolation and molecular characterization of newly emerging avian reovirus variants and novel strains in Pennsylvania, USA, 2011-2014. *Sci. Rep.* (2015) doi:10.1038/srep14727.

13. Bodelón, G., Labrada, L., Martønez-Costas, J. & Benavente, J. The avian reovirus genome segment S1 is a functionally tricistronic gene that expresses One structural and two nonstructural proteins in infected cells. *Virology* (2001) doi:10.1006/viro.2001.1159.

14. Kozak, R. A. *et al.* Replication and oncolytic activity of an avian orthoreovirus in human hepatocellular carcinoma cells. *Viruses* (2017) doi:10.3390/v9040090.

15. Roulstone, V. *et al.* Synergistic cytotoxicity of oncolytic reovirus in combination with cisplatin-paclitaxel doublet chemotherapy. *Gene Ther.* (2013) doi:10.1038/gt.2012.68.

16. Costas, C., Martinez-Costas, J., Bodelon, G. & Benavente, J. The Second Open Reading Frame of the Avian Reovirus S1 Gene Encodes a Transcription-Dependent and CRM1-Independent Nucleocytoplasmic Shuttling Protein. *J. Virol.* **79**, 2141–2150 (2005).

17.   Liu, H. J., Lin, P. Y., Lee, J. W., Hsu, H. Y. & Shih, W. L. Retardation of cell growth by avian reovirus p17 through the activation of p53 pathway. *Biochem. Biophys. Res. Commun.***336**, 709–715 (2005).

18.   Huang, W. R. *et al.* Avian reovirus p17 and σa act cooperatively to downregulate Akt by suppressing mTORC2 and CDK2/cyclin A2 and upregulating proteasome PSMB6. *Sci. Rep.***7**, 1–19 (2017).

19.   Huang, W. R. *et al.* Avian reovirus protein p17 functions as a nucleoporin Tpr suppressor leading to activation of p53, p21 and PTEN and inactivation of PI3K/AKT/mTOR and ERK signaling pathways. *PLoS One***10**, 1–31 (2015).

20.   Chiu, H. C. *et al.*Mechanistic insights into avian reovirus p17-modulated suppression of cell cycle CDK-cyclin complexes and enhancement of p53 and cyclin H interaction. Journal of Biological Chemistry vol. 293 (2018).

21.   Chiu, H. C. *et al.* Suppression of vimentin phosphorylation by the Avian reovirus p17 through Inhibition of CDK1 and Plk1 impacting the G2/M phase of the cell cycle. *PLoS One* (2016) doi:10.1371/journal.pone.0162356.

22.   Hobbs, W. E. & DeLuca, N. A. Perturbation of cell cycle progression and cellular gene expression as a function of herpes simplex virus ICP0. *J. Virol.* (1999).

23.   Lomonte, P. & Everett, R. D. Herpes simplex virus type 1 immediate-early protein Vmw110 inhibits progression of cells through mitosis and from G1 into S phase of the cell cycle. *J. Virol.* (1999).

24.   Cayrol, C. & Flemington, E. K. The Epstein-Barr virus bZIP transcription factor Zta causes G0/G1 cell cycle arrest through induction of cyclin-dependent kinase inhibitors. *EMBO J.* (1996) doi:10.1002/j.1460-2075.1996.tb00635.x.

25.   Chen, C.-J., Sugiyama, K., Kubo, H., Huang, C. & Makino, S. Murine Coronavirus Nonstructural Protein p28 Arrests Cell Cycle in G0/G1 Phase. *J. Virol.* (2004) doi:10.1128/jvi.78.19.10410-10419.2004.

26.   Sieburg, M., Tripp, A., Ma, J.-W. & Feuer, G. Human T-Cell Leukemia Virus Type 1 (HTLV-1) and HTLV-2 Tax Oncoproteins Modulate Cell Cycle Progression and Apoptosis. *J. Virol.* (2004) doi:10.1128/jvi.78.19.10399-10409.2004.

27.   Caccuri, F. *et al.* U94 of human herpesvirus 6 down-modulates Src, promotes a partial mesenchymal-to-epithelial transition and inhibits tumor cell growth, invasion and metastasis. *Oncotarget* **8**, 44533–44549 (2017).

28.   L.M. Sherwood, E.E. Parris, J. Folkman, Tumor Angiogenesis: Therapeutic Implications, N. Engl. J. Med. (1971). https://doi.org/10.1056/NEJM197111182852108.

29.   Shmulevitz, M. & Duncan, R. A new class of fusion-associated small transmembrane (FAST) proteins encoded by the non-enveloped fusogenic reoviruses. *EMBO J.* (2000) doi:10.1093/emboj/19.5.902.

30.   Bodelón, G., Labrada, L., Mart́nez-Costas, J. & Benavente, J. Modification of late membrane permeability in avian reovirus-infected cells. Viroporin activity of the S1-encoded nonstructural p10 protein. *J. Biol. Chem.* (2002) doi:10.1074/jbc.M202018200.

31.   Liu, H. J. *et al.* Activation of small GTPases RhoA and Rac1 is required for Avian Reovirus p10-induced syncytium formation. *Mol. Cells* (2008).

32.   Shapouri, M. R. S., Arella, M. & Silim, A. Evidence for the multimeric nature and cell binding ability of avian reovirus σ3 protein. *J. Gen. Virol.* (1996) doi:10.1099/0022-1317-

77-6-1203.

33. Shih, W. L., Hsu, H. W., Liao, M. H., Lee, L. H. & Liu, H. J. Avian reovirus σC protein induces apoptosis in cultured cells. *Virology* (2004) doi:10.1016/j.virol.2003.12.004.

34. Chen, Y. T., Lin, C. H., Ji, W. T., Li, S. K. & Liu, H. J. Proteasome inhibition reduces avian reovirus replication and apoptosis induction in cultured cells. *J. Virol. Methods* (2008) doi:10.1016/j.jviromet.2008.03.016.

35. Lin, P. Y. *et al.* Modulation of p53 by mitogen-activated protein kinase pathways and protein kinase C δ during avian reovirus S1133-induced apoptosis. *Virology* (2009) doi:10.1016/j.virol.2008.12.028.

36. Chiu, H.-C. *et al.* Heterogeneous Nuclear Ribonucleoprotein A1 and Lamin A/C Modulate Nucleocytoplasmic Shuttling of Avian Reovirus p17. *J. Virol.* (2019) doi:10.1128/jvi.00851-19.

37. Ji, W. T., Wang, L., Lin, R. C., Huang, W. R. & Liu, H. J. Avian reovirus influences phosphorylation of several factors involved in host protein translation including eukaryotic translation elongation factor 2 (eEF2) in Vero cells. *Biochem. Biophys. Res. Commun.* (2009) doi:10.1016/j.bbrc.2009.04.116.

38. Li, C. *et al.* Nuclear localization of the p17 protein of avian reovirus is correlated with autophagy induction and an increase in viral replication. *Arch. Virol.* (2015) doi:10.1007/s00705-015-2598-5.

39. Chi, P. I., Huang, W. R., Lai, I. H., Cheng, C. Y. & Liu, H. J. The p17 nonstructural protein of avian reovirus triggers autophagy enhancing virus replication via activation of phosphatase and tensin deleted on chromosome 10 (PTEN) and AMP-activated protein kinase (AMPK), as well as dsRNA-dependent protein kinase (PKR. *J. Biol. Chem.* 288, 3571–3584 (2013).

40. Theophilos, M. B., Huang, J. A. & Holmes, I. H. Avian reovirus σC protein contains a putative fusion sequence and induces fusion when expressed in mammalian cells. *Virology* (1995) doi:10.1006/viro.1995.1199.

41. Mazzuca, P. *et al.* Role of Autophagy in HIV-1 Matrix Protein p17-Driven Lymphangiogenesis. *J. Virol.* (2017) doi:10.1128/jvi.00801-17.

42. Angelova, A. L., Geletneky, K., Nüesch, J. P. F. & Rommelaere, J. Tumor selectivity of oncolytic parvoviruses: From in vitro and animal models to cancer patients. *Frontiers in Bioengineering and Biotechnology* (2015) doi:10.3389/fbioe.2015.00055.

43. Cornelis, J. J., Salomé, N., Dinsart, C. & Rommelaere, J. Vectors based on autonomous parvoviruses: Novel tools to treat cancer? *Journal of Gene Medicine* (2004) doi:10.1002/jgm.502.

44. Moehler, M. *et al.* Oncolytic parvovirus H1 induces release of heat-shock protein HSP72 in susceptible human tumor cells but may not affect primary immune cells. *Cancer Gene Ther.* (2003) doi:10.1038/sj.cgt.7700591.

45. Hristov, G. *et al.* Through Its Nonstructural Protein NS1, Parvovirus H-1 Induces Apoptosis via Accumulation of Reactive Oxygen Species. *J. Virol.* (2010) doi:10.1128/jvi.01797-09.

46. Wyatt, J., Müller, M. M. & Tavassoli, M. Cancer treatment goes viral: Using viral proteins to induce tumour-specific cell death. *Cancers* (2019) doi:10.3390/cancers11121975.

47. Wang, Y. Y. *et al.* Effect of the parvovirus H-1 non-structural protein NS1 on the

tumorigenicity of human gastric cancer cells. *J. Dig. Dis.* (2012) doi:10.1111/j.1751-2980.2012.00601.x.

48.   Op De Beeck, A. *et al.* NS1- and Minute Virus of Mice-Induced Cell Cycle Arrest: Involvement of p53 and p21cip1. *J. Virol.* (2001) doi:10.1128/jvi.75.22.11071-11078.2001.

49.   Bretscher, C. & Marchini, A. H-1 parvovirus as a cancer-killing agent: Past, present, and future. *Viruses* (2019) doi:10.3390/v11060562.

50.   Berns, K. I. & Labow, M. A. Parvovirus gene regulation. *Journal of General Virology* (1987) doi:10.1099/0022-1317-68-3-601.

51.   Heilbronn, R., Bürkle, A., Stephan, S. & zur Hausen, H. The adeno-associated virus rep gene suppresses herpes simplex virus-induced DNA amplification. *J. Virol.* (1990) doi:10.1128/jvi.64.6.3012-3018.1990.

52.   Di Pasquale, G. & Stacey, S. N. Adeno-Associated Virus Rep78 Protein Interacts with Protein Kinase A and Its Homolog PRKX and Inhibits CREB-Dependent Transcriptional Activation. *J. Virol.* (1998) doi:10.1128/jvi.72.10.7916-7925.1998.

53.   Schlehofer, J. R. The tumor suppressive properties of adeno-associated viruses. *Mutation Research - Fundamental and Molecular Mechanisms of Mutagenesis* (1994) doi:10.1016/0027-5107(94)90250-X.

54.   Batchu, R. B., Shammas, M. A., Wang, J. Y. & Munshi, N. C. Interaction of adeno-associated virus Rep78 with p53: Implications in growth inhibition. *Cancer Res.* (1999).

55.   Prasad, C. K. *et al.* The adeno-associated virus major regulatory protein Rep78-c-Jun-DNA motif complex modulates AP-1 activity. *Virology* (2003) doi:10.1016/S0042-6822(03)00439-2.

56.   Berthet, C., Raj, K., Saudan, P. & Beard, P. How adeno-associated virus Rep78 protein arrests cells completely in S phase. *Proc. Natl. Acad. Sci. U. S. A.* (2005) doi:10.1073/pnas.0504583102.

57.   Alam, S. *et al.* Adeno-associated virus type 2 infection activates caspase dependent and independent apoptosis in multiple breast cancer lines but not in normal mammary epithelial cells. *Mol. Cancer* (2011) doi:10.1186/1476-4598-10-97.

58.   Rapp, J. C., Krug, L. T., Inoue, N., Dambaugh, T. R. & Pellett, P. E. U94, the human herpesvirus 6 homolog of the parvovirus nonstructural gene, is highly conserved among isolates and is expressed at low mRNA levels as a spliced transcript. *Virology* (2000) doi:10.1006/viro.1999.0163.

59.   Rotola, A. *et al.* U94 of human herpesvirus 6 is expressed in latently infected peripheral blood mononuclear cells and blocks viral gene expression in transformed lymphocytes in culture. *Proc. Natl. Acad. Sci. U. S. A.* (1998) doi:10.1073/pnas.95.23.13911.

60.   Rizzo, R. *et al.* Human Herpesvirus 6A and 6B inhibit in vitro angiogenesis by induction of Human Leukocyte Antigen G. *Sci. Rep.* (2018) doi:10.1038/s41598-018-36146-0.

61.   Matheeussen, V. *et al.* Expression and spatial heterogeneity of dipeptidyl peptidases in endothelial cells of conduct vessels and capillaries. *Biol. Chem.* (2011) doi:10.1515/BC.2011.002.

62.   Ansorge, S. *et al.* Novel aspects of cellular action of dipeptidyl peptidase IV/CD26. *Biol. Chem.* (2011) doi:10.1515/BC.2011.008.

63.   Korkmaz, H. I. *et al.* Homocysteine-induced inverse expression of tissue factor and DPP4

in endothelial cells is related to NADPH oxidase activity. *Physiol. Int.* (2019) doi:10.1556/2060.106.2019.05.

64. De Nigris, V. D. *et al.* Teneligliptin enhances the beneficial effects of GLP-1 in endothelial cells exposed to hyperglycemic conditions. *Oncotarget* (2018) doi:10.18632/oncotarget.22849.

65. Röhrborn, D., Eckel, J. & Sell, H. Shedding of dipeptidyl peptidase 4 is mediated by metalloproteases and up-regulated by hypoxia in human adipocytes and smooth muscle cells. *FEBS Lett.* (2014) doi:10.1016/j.febslet.2014.08.029.

66. A. Caruso, F. Favilli, A. Rotola, M. Comar, D. Horejsh, G. Alessandri, M. Grassi, D. Di Luca, S. Fiorentini, Human herpesvirus-6 modulates RANTES production in primary human endothelial cell cultures, J. Med. Virol. (2003). https://doi.org/10.1002/jmv.10416.

67. F. Caccuri, C. Giagulli, A. Bugatti, A. Benetti, G. Alessandri, D. Ribatti, S. Marsico, P. Apostoli, M.A. Slevin, M. Rusnati, C.A. Guzman, S. Fiorentini, A. Caruso, HIV-1 matrix protein p17 promotes angiogenesis via chemokine receptors CXCR1 and CXCR2, Proc. Natl. Acad. Sci. U. S. A. (2012). https://doi.org/10.1073/pnas.1206605109.

68. R. Ronca, P. Benzoni, D. Leali, C. Urbinati, M. Belleri, M. Corsini, P. Alessi, D. Coltrini, S. Calza, M. Presta, P. Dell'Era, Antiangiogenic activity of a neutralizing human single-chain antibody fragment against fibroblast growth factor receptor 1, Mol. Cancer Ther. (2010). https://doi.org/10.1158/1535-7163.MCT-10-0417.

69. S. Mitola, E. Moroni, C. Ravelli, G. Andres, M. Belleri, M. Presta, Angiopoietin-1 mediates the proangiogenic activity of the bone morphogenic protein antagonist Drm, Blood. (2008). https://doi.org/10.1182/blood-2007-09-111450.

70. A.M. Laib, A. Bartol, A. Alajati, T. Korff, H. Weber, H.G. Augustin, Spheroid-based human endothelial cell microvessel formation in vivo, Nat. Protoc. (2009). https://doi.org/10.1038/nprot.2009.96.

71. M. Malumbres, M. Barbacid (2007) Cell cycle kinases in cancer. Curr Opin Genet Dev 17: 60-65. https://doi.org/10.1016/j.gde.2006.12.008

72. D.W. Heilman, J.G. Teodoro, M.R. Green (2006) Apoptin Nucleocytoplasmic Shuttling Is Required for Cell Type-Specific Localization, Apoptosis, and Recruitment of the Anaphase-Promoting Complex/Cyclosome to PML Bodies. J Virol 80:7535-45https://doi.org/10.1128/JVI.02741-05

73. Q. Wang, X. Yuan, Y. Chen, Q. Zheng, L. Xu, Y. Wu (2018) Endoplasmic reticulum stress mediated MDRV p10.8 protein-induced cell cycle arrest and apoptosis through the PERK/eIF2α pathway. Front Microbiol 9:1327https://doi.org/10.3389/fmicb.2018.01327

74. M.L.Li , V. Stollar (2004) Alphaviruses and apoptosis.Int Rev Immunol 23:7-24 https://doi.org/10.1080/08830180490265529

75. W.C.M. Dempke, V. Heinemann, Resistance to EGF-R (erbB-1) and VEGF-R modulating agents, Eur. J. Cancer. (2009). https://doi.org/10.1016/j.ejca.2008.11.038.

76. N. Ferrara, VEGF and the quest for tumour angiogenesis factors, Nat. Rev. Cancer. (2002). https://doi.org/10.1038/nrc909.

77. J. Huang, J.S. Frischer, A. Serur, A. Kadenhe, A. Yokoi, K.W. McCrudden, T. New, K. O'Toole, S. Zabski, J.S. Rudge, J. Holash, G.D. Yancopoulos, D.J. Yamashiro, J.J. Kandel, Regression of established tumors and metastases by potent vascular endothelial growth factor blockade, Proc. Natl. Acad. Sci. U. S. A. (2003). https://doi.org/10.1073/pnas.1432908100.

78. K. De Bock, M. Mazzone, P. Carmeliet, Antiangiogenic therapy, hypoxia, and metastasis:

Risky liaisons, or not?, Nat. Rev. Clin. Oncol. (2011). https://doi.org/10.1038/nrclinonc.2011.83.

79. A. Zubilewicz, C. Hecquet, J.C. Jeanny, G. Soubrane, Y. Courtois, F. Mascarelli, Two distinct signalling pathways are involved in FGF2-stimulated proliferation of choriocapillary endothelial cells: A comparative study with VEGF, Oncogene. (2001). https://doi.org/10.1038/sj.onc.1204231.

80. O. Casanovas, D.J. Hicklin, G. Bergers, D. Hanahan, Drug resistance by evasion of antiangiogenic targeting of VEGF signaling in late-stage pancreatic islet tumors, Cancer Cell. (2005). https://doi.org/10.1016/j.ccr.2005.09.005.

81. R.N. Gacche, Compensatory angiogenesis and tumor refractoriness, Oncogenesis. (2015). https://doi.org/10.1038/oncsis.2015.14.

82. I.S. Babina, N.C. Turner, Advances and challenges in targeting FGFR signalling in cancer, Nat. Rev. Cancer. (2017). https://doi.org/10.1038/nrc.2017.8.

83. K. Garber, Angiogenesis inhibitors suffer new setback, Nat. Biotechnol. (2002). https://doi.org/10.1038/nbt1102-1067.

84. N.H.D. Pamela A. Havre1, Masako Abe1, Yasuyo Urasaki1, Kei Ohnuma2, Chikao Morimoto2, The role of CD26/dipeptidyl peptidase IV in cancer, Front. Biosci. 13 (2008) 1634–1645.

85. O.J. Cordero, F.J. Salgado, M. Nogueira, On the origin of serum CD26 and its altered concentration in cancer patients, Cancer Immunol. Immunother. (2009). https://doi.org/10.1007/s00262-009-0728-1.

86. A. Erić-Nikolić, I.Z. Matić, M. Dordević, Z. Milovanović, I. Marković, R. Džodić, M. Inić, T. Srdić-Rajić, M. Jevrić, D. Gavrilović, O.J. Cordero, Z.D. Juranić, Serum DPPIV activity and CD26 expression on lymphocytes in patients with benign or malignant breast tumors, Immunobiology. (2011). https://doi.org/10.1016/j.imbio.2011.01.005.

87. A. Beckenkamp, J.B. Willig, D.B. Santana, J. Nascimento, J.D. Paccez, L.F. Zerbini, A.N. Bruno, D.A. Pilger, M.R. Wink, A. Buffon, Differential expression and enzymatic activity of DPPIV/CD26 affects migration ability of cervical carcinoma cells, PLoS One. (2015). https://doi.org/10.1371/journal.pone.0134305.

88. T. Nargis, K. Kumar, A.R. Ghosh, A. Sharma, D. Rudra, D. Sen, S. Chakrabarti, S. Mukhopadhyay, D. Ganguly, P. Chakrabarti, KLK5 induces shedding of DPP4 from circulatory Th17 cells in type 2 diabetes, Mol. Metab. (2017). https://doi.org/10.1016/j.molmet.2017.09.004.

89. A.M. Lambeir, C. Durinx, S. Scharpé, I. De Meester, Dipeptidyl-peptidase IV from bench to bedside: An update on structural properties, functions, and clinical aspects of the enzyme DPP IV, Crit. Rev. Clin. Lab. Sci. (2003). https://doi.org/10.1080/713609354.

90. A.M. Lambeir, P. Proost, C. Durinx, G. Bal, K. Senten, K. Augustyns, S. Scharpé, J. Van Dammes, I. De Meester, Kinetic Investigation of Chemokine Truncation by CD26/Dipeptidyl Peptidase IV Reveals a Striking Selectivity within the Chemokine Family, J. Biol. Chem. (2001). https://doi.org/10.1074/jbc.M103106200.

91. A. Beckenkamp, S. Davies, J.B. Willig, A. Buffon, DPPIV/CD26: a tumor suppressor or a marker of malignancy?, Tumor Biol. (2016). https://doi.org/10.1007/s13277-016-5005-2.

92. Y.X. Sun, E.A. Pedersen, Y. Shiozawa, A.M. Havens, Y. Jung, J. Wang, K.J. Pienta, R.S. Taichman, CD26/dipeptidyl peptidase IV regulates prostate cancer metastasis by degrading SDF-1/CXCL12, Clin. Exp. Metastasis. 25 (2008) 765–776. https://doi.org/10.1007/s10585-008-9188-9.

93.   W.T. Arscott, A.E. LaBauve, V. May, U. V. Wesley, Suppression of neuroblastoma growth by dipeptidyl peptidase IV: Relevance of chemokine regulation and caspase activation, Oncogene. 28 (2009) 479–491. https://doi.org/10.1038/onc.2008.402.

94.   U. V. Wesley, S. Tiwari, A.N. Houghton, Role for dipeptidyl peptidase IV in tumor suppression of human non small cell lung carcinoma cells, Int. J. Cancer. (2004). https://doi.org/10.1002/ijc.20091.

95.   H. Kajiyama, K. Shibata, M. Terauchi, K. Ino, A. Nawa, F. Kikkawa, Involvement of DPPIV/CD26 in epithelial morphology and suppressed invasive ability in ovarian carcinoma cells, Ann. N. Y. Acad. Sci. 1086 (2006) 233–240. https://doi.org/10.1196/annals.1377.007.

96.   F. Yang, Y. Takagaki, Y. Yoshitomi, T. Ikeda, J. Li, M. Kitada, A. Kumagai, E. Kawakita, S. Shi, K. Kanasaki, D. Koya, Inhibition of dipeptidyl peptidase-4 accelerates epithelial–mesenchymal transition and breast cancer metastasis via the CXCL12/CXCR4/mTOR axis, Cancer Res. 79 (2019) 735–746. https://doi.org/10.1158/0008-5472.CAN-18-0620.

97.   M.G. Narducci, E. Scala, A. Bresin, E. Caprini, M.C. Picchio, D. Remotti, G. Ragone, F. Nasorri, M. Frontani, D. Arcelli, S. Volinia, G.A. Lombardo, G. Baliva, M. Napolitano, G. Russo, Skin homing of Sézary cells involves SDF-1-CXCR4 signaling and down-regulation of CD26/dipeptidylpeptidase IV, Blood. (2006). https://doi.org/10.1182/blood-2005-04-1492.

98.   L. É.C., B. J., The dietary flavonoid apigenin enhances the activities of the anti-metastatic protein CD26 on human colon carcinoma cells, Clin. Exp. Metastasis. (2011).

99.   P. Proost, S. Struyf, D. Schols, C. Durinx, A. Wuyts, J.P. Lenaerts, E. De Clercq, I. De Meester, J. Van Damme, Processing by CD26/dipeptidyl-peptidase IV reduces the chemotactic and anti-HIV-1 activity of stromal-cell-derived factor-1α, FEBS Lett. (1998). https://doi.org/10.1016/S0014-5793(98)00830-8.

100.   T. Shioda, H. Kato, Y. Ohnishi, K. Tashiro, M. Ikegawa, E.E. Nakayama, H. Hu, A. Kato, Y. Sakai, H. Liu, T. Honjo, A. Nomoto, A. Iwamoto, C. Morimoto, Y. Nagai, Anti-HIV-1 and chemotactic activities of human stromal cell-derived factor 1α (SDF-1α) and SDF-1β are abolished by CD26/dipeptidyl peptidase IV-mediated cleavage, Proc. Natl. Acad. Sci. U. S. A. (1998). https://doi.org/10.1073/pnas.95.11.6331.

101.   P. Busek, J. Stremenova, L. Sromova, M. Hilser, E. Balaziova, D. Kosek, J. Trylcova, H. Strnad, E. Krepela, A. Sedo, Dipeptidyl peptidase-IV inhibits glioma cell growth independent of its enzymatic activity, Int. J. Biochem. Cell Biol. (2012). https://doi.org/10.1016/j.biocel.2012.01.011.

102.   Y. Mizokami, H. Kajiyama, K. Shibata, K. Ino, F. Kikkawa, S. Mizutani, Stromal cell-derived factor-1α-induced cell proliferation and its possible regulation by CD26/dipeptidyl peptidase IV in endometrial adenocarcinoma, Int. J. Cancer. (2004). https://doi.org/10.1002/ijc.20183.

103.   F. Kikkawa, H. Kajiyama, K. Shibata, K. Ino, S. Nomura, S. Mizutani, Dipeptidyl peptidase IV in tumor progression, in: Biochim. Biophys. Acta - Proteins Proteomics, 2005. https://doi.org/10.1016/j.bbapap.2004.09.028.

104.   U. V. Wesley, M. McGroarty, A. Homoyouni, Dipeptidyl peptides inhibits malignant phenotype of prostate cancer cells by blocking basic fibroblast growth factor signaling pathway, Cancer Res. (2005). https://doi.org/10.1158/0008-5472.CAN-04-1852.

105.   K. Kishimoto, S. Liu, T. Tsuji, K.A. Olson, G.F. Hu, Endogenous angiogenin in

endothelial cells is a general requirement for cell proliferation and angiogenesis, Oncogene. (2005). https://doi.org/10.1038/sj.onc.1208223.

106. S. De Falco, The discovery of placenta growth factor and its biological activity, Exp. Mol. Med. (2012). https://doi.org/10.3858/emm.2012.44.1.025.

107. Schat KA. 2009. Chicken anemia virus. Curr Top Microbiol Immunol.

108. Todd D. 2000. Circoviruses: Immunosuppressive threats to avian species: A review. Avian Pathol.

109. Jeurissen SH, Wagenaar F, Pol JM, van der Eb AJ, Noteborn MH. 1992. Chicken anemia virus causes apoptosis of thymocytes after in vivo infection and of cell lines after in vitro infection. J Virol.

110. Leliveld SR, Dame RT, Rohn JL, Noteborn MHM, Abrahams JP. 2004. Apoptin's functional N- and C-termini independently bind DNA. FEBS Lett.

111. Heilman DW, Teodoro JG, Green MR. 2006. Apoptin Nucleocytoplasmic Shuttling Is Required for Cell Type-Specific Localization, Apoptosis, and Recruitment of the Anaphase-Promoting Complex/Cyclosome to PML Bodies. J Virol.

112. Danen-Van Oorschot AAAM, Zhang YH, Leliveld SR, Rohn JL, Seelen MCMJ, Bolk MW, Van Zon A, Erkeland SJ, Abrahams JP, Mumberg D, Noteborn MHM. 2003. Importance of nuclear localization of apoptin for tumor-specific induction of apoptosis. J Biol Chem.

113. Rohn JL, Zhang YH, Aalbers RIJM, Otto N, Den Hertog J, Henriquez N V., Van de Velde CJH, Kuppen PJK, Mumberg D, Donner P, Noteborn MHM. 2002. A tumor-specific kinase activity regulates the viral death protein apoptin. J Biol Chem.

114. Lee YH, Cheng CM, Chang YF, Wang TY, Yuo CY. 2007. Apoptin T108 phosphorylation is not required for its tumor-specific nuclear localization but partially affects its apoptotic activity. Biochem Biophys Res Commun.

115. Maddika S, Booy EP, Johan D, Gibson SB, Ghavami S, Los M. 2005. Cancer-specific toxicity of apoptin is independent of death receptors but involves the loss of mitochondrial membrane potential and the release of mitochondrial cell-death mediators by a Nurr77-dependent pathway. J Cell Sci.

116. Danen-van Oorschot AAAM, van der Eb AJ, Noteborn MHM. 2000. The Chicken Anemia Virus-Derived Protein Apoptin Requires Activation of Caspases for Induction of Apoptosis in Human Tumor Cells. J Virol.

117. Taebunpakul P, Sayan BS, Flinterman M, Klanrit P, Gäken J, Odell EW, Melino G, Tavassoli M. 2012. Apoptin induces apoptosis by changing the equilibrium between the stability of TAp73 and DNp73 isoforms through ubiquitin ligase PIR2. Apoptosis.

118. Klanrit P, Flinterman MB, Odell EW, Melino G, Killick R, Norris JS, Tavassoli M. 2008. Specific isoforms of p73 control the induction of cell death induced by the viral proteins, E1A or apoptin. Cell Cycle.

119. Kucharski TJ, Gamache I, Gjoerup O, Teodoro JG. 2011. DNA Damage Response Signaling Triggers Nuclear Localization of the Chicken Anemia Virus Protein Apoptin. J Virol.

120. Thomas J. Kucharski, Timothy F. Ng, David M. Sharon, Pedram Navid-Azarbaijani, Mahvash Tavassoli JGT. 2016. Activation of the Chicken Anemia Virus Apoptin Protein by Chk1/2 Phosphorylation Is Required for Apoptotic Activity and Efficient Viral Replication. J Virol 90:9433–9445.

121. Maddika S, Bay GH, Kroczak TJ, Ande SR, Maddika S, Wiechec E, Gibson SB, Los M.

2007. Akt is transferred to the nucleus of cells treated with apoptin, and it participates in apoptin-induced cell death. Cell Prolif.

122. Bullenkamp J, Gäken J, Festy F, Chong EZ, Ng T, Tavassoli M. 2015. Apoptin interacts with and regulates the activity of protein kinase C beta in cancer cells. Apoptosis.

123. Murray NR, Davidson LA, Chapkin RS, Gustafson WC, Schattenberg DG, Fields AP. 1999. Overexpression of protein kinase C β(II) induces colonic hyperproliferation and increased sensitivity to colon carcinogenesis. J Cell Biol.

124. Gökmen-Polar Y, Murray NR, Velasco MA, Gatalica Z, Fields AP. 2001. Elevated protein kinase C βII is an early promotive event in colon carcinogenesis. Cancer Res.

125. Holler C, Pinon JD, Denk U, Heyder C, Hofbauer S, Greil R, Egle A. 2009. PKC{beta} is essential for the development of CLL in the TCL1 transgenic mouse model: Validation of PKC{beta} as a therapeutic target in CLL. Blood.

126. Panigrahi S, Stetefeld J, Jangamreddy JR, Mandal S, Mandal SK, Los M. 2012. Modeling of molecular interaction between apoptin, BCR-Abl and CrKL - an alternative approach to conventional rational drug design. PLoS One.

127. Jangamreddy JR, Panigrahi S, Lotfi K, Yadav M, Maddika S, Tripathi AK, Sanyal S, Los MJ. 2014. Mapping of Apoptin-interaction with BCR-ABL1, and development of apoptin-based targeted therapy. Oncotarget.

128. Zhang L, Zhao H, Cui Z, Lv Y, Zhang W, Ma X, Zhang J, Sun B, Zhou D, Yuan L. 2017. A peptide derived from apoptin inhibits glioma growth. Oncotarget.

129. Hou Z, Mao J, Lu Y, Li L. 2018. rApoptin induces apoptosis in human breast cancer cells via phosphorylation of Nur77 and Akt. Biochem Biophys Res Commun.

130. Burek M, Maddika S, Burek CJ, Daniel PT, Schulze-Osthoff K, Los M. 2006. Apoptin-induced cell death is modulated by Bcl-2 family members and is Apaf-1 dependent. Oncogene.

131. Yuan L, Zhao H, Zhang L, Liu X. 2013. The efficacy of combination therapy using adeno-associated virus-mediated co-expression of apoptin and interleukin-24 on hepatocellular carcinoma. Tumor Biol.

132. Song W, Zhao H, Cui Z, Ma X, Zhang W, Wang D, Liu A, Yuan L. 2016. Creation of an apoptin-derived peptide that interacts with SH3 domains and inhibits glioma cell migration and invasion. Tumor Biol.

133. Zhou D, Liu W, Liang S, Sun B, Liu A, Cui Z, Han X, Yuan L. 2018. Apoptin-derived peptide reverses cisplatin resistance in gastric cancer through the PI3K–AKT signaling pathway. Cancer Med.

134. Wang Q, Yuan X, Chen Y, Zheng Q, Xu L, Wu Y. 2018. Endoplasmic reticulum stress mediated MDRV p10.8 protein-induced cell cycle arrest and apoptosis through the PERK/eIF2α pathway. Front Microbiol.

135. Wu Y, Cui L, Zhu E, Zhou W, Wang Q, Wu X, Wu B, Huang Y, Liu HJ. 2017. Muscovy duck reovirus σnS protein triggers autophagy enhancing virus replication. Virol J.

136. Guo D, Qiu N, Shaozhou W, Bai X, He Y, Zhang Q, Zhao J, Liu M, Zhang Y. 2014. Muscovy duck reovirus p10.8 protein localizes to the nucleus via a nonconventional nuclear localization signal. Virol J.

137. Geng H, Zhang Y, Liu-Partanen Y, Vanhanseng, Guo D, Wang Y, Liu M, Tong G. 2009. Apoptosis Induced by Duck Reovirus P10.8 Protein in Primary Duck Embryonated Fibroblast and Vero E6 Cells. Avian Dis Dig.

138. Chulu JLC, Lee LH, Lee YC, Liao SH, Lin FL, Shih WL, Liu HJ. 2007. Apoptosis

induction by avian reovirus through p53 and mitochondria-mediated pathway. Biochem Biophys Res Commun.

139. Lin PY, Liu HJ, Chang CD, Chen YC, Chang CI SW. 2015. Avian reovirus S1133-induced apoptosis is associated with Bip/GRP79-mediated Bim translocation to the endoplasmic reticulum. Apoptosis 481–490.

140. Wang Q, Liu M, Chen Y, Xu L, Wu B, Wu Y, Huang Y, Huang WR, Liu HJ. 2019. Muscovy duck reovirus p10.8 protein induces ER stress and apoptosis through the Bip/IRE1/XBP1 pathway. Vet Microbiol.

141. Wang Q, Huang WR, Chih WY, Chuang KP, Chang CD, Wu Y, Huang Y, Liu HJ. 2019. Cdc20 and molecular chaperone CCT2 and CCT5 are required for the Muscovy duck reovirus p10.8-induced cell cycle arrest and apoptosis. Vet Microbiol.

142.   Strauss JH, Strauss EG. 1994. The alphaviruses: Gene expression, replication, and evolution. Microbiol Rev.

143. Akhrymuk I, Frolov I, Frolova EI. 2018. Sindbis Virus Infection Causes Cell Death by nsP2-Induced Transcriptional Shutoff or by nsP3-Dependent Translational Shutoff. J Virol.

144. Choi Y, Chang J. 2013. Viral vectors for vaccine applications. Clin Exp Vaccine Res.

145. Unno Y, Shino Y, Kondo F, Igarashi N, Wang G, Shimura R, Yamaguchi T, Asano T, Saisho H, Sekiya S, Shirasawa H. 2005. Oncolytic viral therapy for cervical and ovarian cancer cells by sindbis virus AR339 strain. Clin Cancer Res.

146. Pratt WD, Fine DL, Hart MK, Martin SS, Reed DS. 2012. AlphavirusesBiodefense Research Methodology and Animal Models, Second Edition.

147. Tseng J-C. 2002. In Vivo Antitumor Activity of Sindbis Viral Vectors. CancerSpectrum Knowl Environ.

148. Saito K, Uzawa K, Kasamatsu A, Shinozuka K, Sakuma K, Yamatoji M, Shiiba M, Shino Y, Shirasawa H, Tanzawa H. 2009. Oncolytic activity of Sindbis virus in human oral squamous carcinoma cells. Br J Cancer.

149. Lundstrom K. 2017. Oncolytic alphaviruses in cancer immunotherapy. Vaccines.

150. Yi R, Saito K, Isegawa N, Shirasawa H. 2015. Alteration of cell cycle progression by Sindbis virus infection. Biochem Biophys Res Commun.

151. Wen JS, Zhao WZ, Liu JW, Zhou H, Tao JP, Yan HJ, Liang Y, Zhou JJ, Jiang LF. 2007. Genomic analysis of a Chinese isolate of Getah-like virus and its phylogenetic relationship with other Alphaviruses. Virus Genes.

152. Brown CM, Timoney PJ. 1998. Getah virus infection of Indian horses. Trop Anim Health Prod.

153. Bick MJ, Carroll J-WN, Gao G, Goff SP, Rice CM, MacDonald MR. 2003. Expression of the Zinc-Finger Antiviral Protein Inhibits Alphavirus Replication. J Virol.

154. Lin Y, Zhang H, Liang J, Li K, Zhu W, Fu L, Wang F, Zheng X, Shi H, Wu S, Xiao X, Chen L, Tang L, Yan M, Yang X, Tan Y, Qiu P, Huang Y, Yin W, Su X, Hu H, Hu J, Yan G. 2014. Identification and characterization of alphavirus M1 as a selective oncolytic virus targeting ZAP-defective human cancers. Proc Natl Acad Sci U S A.

155. Zhang H, Lin Y, Li K, Liang J, Xiao X, Cai J, Tan Y, Xing F, Mai J, Li Y, Chen W, Sheng L, Gu J, Zhu W, Yin W, Qiu P, Su X, Lu B, Tian X, Liu J, Lu W, Dou Y, Huang Y, Hu B, Kang Z, Gao G, Mao Z, Cheng SY, Lu L, Bai XT, Gong S, Yan G, Hu J. 2016. Naturally Existing Oncolytic Virus M1 Is Nonpathogenic for the Nonhuman Primates after Multiple Rounds of Repeated Intravenous Injections. Hum Gene Ther.

156. Urban C, Rhême C, Maerz S, Berg B, Pick R, Nitschke R, Borner C. 2008. Apoptosis induced by Semliki Forest virus is RNA replication dependent and mediated via Bak. Cell Death Differ.

157. Saito EY, Saito K, Hishiki T, Takenouchi A, Saito T, Sato Y, Terui K, Matsunaga T, Shirasawa H, Yoshida H. 2020. Sindbis viral structural protein cytotoxicity on human neuroblastoma cells. Pediatr Surg Int 36:1173–1180.

158. Gaedigk-Nitschko K, Schlesinger MJ. 1991. Site-directed mutations in sindbis virus E2 glycoprotein's cytoplasmic domain and the 6K protein lead to similar defects in virus assembly and budding. Virology.

159. Sawicki DL, Perri S, Polo JM, Sawicki SG. 2006. Role for nsP2 Proteins in the Cessation of Alphavirus Minus-Strand Synthesis by Host Cells. J Virol.

160. Tamm K, Merits A, Sarand I. 2008. Mutations in the nuclear localization signal of nsP2 influencing RNA synthesis, protein expression and cytotoxicity of Semliki Forest virus. J Gen Virol.

161. Li ML, Stollar V. 2004. Alphaviruses and apoptosis. Int Rev Immunol.

162. Glasgow GM, McGee MM, Tarbatt CJ, Mooney DA, Sheahan BJ, Atkins GJ. 1998. The Semliki Forest virus vector induces p53-independent apoptosis. J Gen Virol.

163. Hurtado A, Tseng JC, Boivin C, Levin B, Yee H, Pampeno C, Meruelo D. 2005. Identification of amino acids of Sindbis virus E2 protein involved in targeting tumor metastases in vivo. Mol Ther.